Journal of Statistical Physics, Vol. 92, Nos. 1/2, 1998

Finite-Size Scaling in the p-State Mean-Field Potts Glass: A Monte Carlo Investigation

O. Dillmann,[1] W. Janke,[1,2] and K. Binder[1]

Received December 3, 1997

The p-state mean-field Potts glass with bimodal bond distribution ($\pm J$) is studied by Monte Carlo simulations, both for $p=3$ and $p=6$ states, for system sizes from $N=5$ to $N=120$ spins, considering particularly the finite-size scaling behavior at the exactly known glass transition temperature T_c. It is shown that for $p=3$ the moments $q^{(k)}$ of the spin-glass order parameter satisfy a simple scaling behavior, $q^{(k)} \propto N^{-k/3} \tilde{f}_k\{N^{1/3}(1-T/T_c)\}$, $k=1, 2, 3, \ldots$, $\tilde{f}_k$ being the appropriate scaling function and T the temperature. Also the specific heat maxima have a similar behavior, $c_V^{\max} \propto \text{const} - N^{-1/3}$, while moments of the magnetization scale as $m^{(k)} \propto N^{-k/2}$. The approach of the positions $T_{\max}$ of these specific heat maxima to T_c as $N \to \infty$ is nonmonotonic. For $p=6$ the results are compatible with a first-order transition, $q^{(k)} \to (q_{\text{jump}})^k$ as $N \to \infty$, but since the order parameter q_{jump} at T_c is rather small, a behavior $q^{(k)} \propto N^{-k/3}$ as $N \to \infty$ also is compatible with the data. Thus no firm conclusions on the finite-size behavior of the order parameter can be drawn. The specific heat maxima $c_V^{\max}$ behave qualitatively in the same way as for $p=3$, consistent with the prediction that there is no latent heat. A speculative phenomenological discussion of finite-size scaling for such transitions is given. For small N ($N \leqslant 15$ for $p=3$, $N \leqslant 12$ for $p=6$) the Monte Carlo data are compared to exact partition function calculations, and excellent agreement is found. We also discuss ratios $R_X \equiv [(\langle X \rangle_T - [\langle X \rangle_T]_{\text{av}})^2]_{\text{av}} / [\langle X \rangle_T]_{\text{av}}^2$, for various quantities X, to test the possible lack of self-averaging at T_c.

KEY WORDS: Mean-field Potts glass; orientational glass; infinite range interactions; Monte Carlo simulations; finite-size scaling; self-averaging; first-order transition without latent heat.

[1] Institut für Physik, Johannes Gutenberg-Universität Mainz, D-55099 Mainz, Germany.
[2] Institut für Theoretische Physik, Universität Leipzig, D-04109 Leipzig, Germany.

0022-4715/98/0700-0057$15.00/0

1. INTRODUCTION

Spin glasses are model systems to elucidate the role of quenched disorder in condensed matter systems and the new types of phase transition phenomena that such materials may show.[1–4]

Most theoretical research was concerned with the Ising spin glasses, where spins $S_i = \pm 1$ interact with randomly chosen pairwise exchange interactions J_{ij}. In the present paper, however, we are concerned with the Potts glass,[5–8] a generalization of the Ising spin glass model to a model with p discrete states, $S_i \in \{1, 2, ..., p\}$, p being an integer. An exchange energy $J_{ij}\delta_{S_iS_j}$ between these Potts spins is nonzero only if the considered pair (i, j) of sites is in the same state, and the value of this energy does not depend on which of the p states the two sites are in, and again J_{ij} is treated as a randomly quenched variable.

The Potts glass is a crude model for anisotropic orientational glasses,[9–11] if we associate the p discrete states with p orientations of an uniaxial molecule in a diluted molecular crystal. (Just as spin glasses result from random dilution of magnetic materials with atoms that carry no magnetic moment, orientational or quadrupolar glasses result from random dilution of molecular crystals with atoms that carry no electric quadrupole moment, e.g., N_2 diluted with Ar.[12]). Thus, $p = 3$ if the molecules can align only along the x, y, z axes of a cubic crystal, $p = 6$ if they can only align along the face diagonals, etc.

The main interest in the Potts glass is not due to applications to these materials, however, but rather due to the fact that the Potts glass is a generic model to learn about the concepts of phase transitions and ordering phenomena in spin glasses, and perhaps in glassy materials in general, similarly as the nearest neighbor Potts ferromagnet is one of the "work horses" for the theory of standard phase transitions.[13] The infinite-range version of the Potts glass has particularly intriguing properties: the transition from the disordered phase to the glass phase is of second order for $p \leqslant 4$, but of first order for $p > 4$. Although in the latter case the glass order parameter at the transition temperature T_c jumps discontinuously from zero to a nonzero value q_{jump}, there is no latent heat,[6] unlike standard first-order transitions. In addition, at a lower temperature T_2 a second transition to a different kind of low temperature spin glass phase occurs, for a certain range of values for the first moment of the bond distribution. Finally, the dynamic version of the mean-field theory of Potts glasses[14, 15] exhibits striking similarities to the mode coupling theory of the glass transition.[16]

Of course, it is a challenging question which of these puzzling properties also occur for short range Potts glasses, and for which spatial

dimensions d. Since for spin glass systems the upper critical dimension d_u, above which mean-field theory holds qualitatively, is commonly believed to be $d_u = 6$,[1, 10] a rather different behavior is expected for physically relevant dimensionalities. But a Monte Carlo study[17] of a nearest neighbor Potts glass with $p = 3$ states has been interpreted in $d = 4$ dimensions as being compatible with a first-order glass transition of similar type as in the infinite-range model. However, only extremely small lattice sizes were accessible in that work,[17] which hence was plagued with finite-size effects, which are not well understood. A systematic study of finite-size effects for such unconventional phase transitions is clearly required before one can meaningfully interpret results as those of ref. 17. In addition, the study of finite-size effects on phase transitions is interesting in its own right,[18, 21] and has contributed a lot to the understanding of phase transitions in general. Indeed the study of finite-size effects in the infinite range Ising spin glass has proven very useful,[22–24] and hence analogous studies of the Potts glass clearly are warranted.

In previous work,[25] a first step in this direction was taken by exact partition function calculations, which could be carried out for $p = 3$ up to $N = 15$, and for $p = 6$ up to $N = 12$. While such sizes clearly are too small to reach the asymptotic limit of finite-size scaling of either model, some valuable hints on the behavior of these models could already be gained. Moreover, this work is very valuable as an independent check on the Monte Carlo simulations that are presented below, which extend from $N = 5$ to $N = 120$. As is well known,[1, 10, 11] Monte Carlo simulations of glassy systems sometimes suffer from an underestimation of the relaxation times at equilibrium, and/or from insufficient size of the sample average over the disordered bond configurations (in a finite-size scaling context the lack of self-averaging is particularly noteworthy[26, 27]). Since the partition function calculations provide exact equilibrium results, and large samples are accessible (up to 10^5 or even 10^6 samples were averaged over ref. 25), these results do validate the procedures used here for equilibration of the data, and justify that the accuracy taken from much smaller samples (only 200 samples are taken in the calculations presented below) actually suffices.

In the next section, we define the model and the quantities that are calculated and give some details on the computational procedures. Section 3 then describes our results for the case $p = 3$, and analyzes them in terms of the finite-size scaling theory that was already sketched in ref. 25. Section 4 presents the results for $p = 6$, where our data confirm the existence of the first order transition without latent heat. Phenomenological discussions of the finite-size scaling behavior of this case are given. Section 5 then summarizes our conclusions.

2. MODEL AND COMPUTATIONAL PROCEDURES

2.1. The Model

The Hamiltonian of the p-state mean-field Potts glass of N interacting Potts spins S_i $(i=1, 2,..., N)$ that can take the p discrete values $S_i=1, 2,..., p$ is defined as[5-11, 25]

$$\mathscr{H} = -p \sum_{i<j} J_{ij}\delta_{S_iS_j} \tag{1}$$

The "exchange constants" (bonds) J_{ij} are quenched random variables, distributed according to a distribution function $P(J_{ij})$, whose first two moments are chosen according to

$$J_0 \equiv [J_{ij}]_{\text{av}} \equiv \tilde{J}_0/(N-1) \tag{2}$$

$$(\Delta J)^2 \equiv [J_{ij}^2]_{\text{av}} - [J_{ij}]_{\text{av}}^2 \equiv \tilde{J}^2/(N-1) \tag{3}$$

Here we denote by $[\cdots]_{\text{av}}$ an average over all realizations of disordered bonds, while thermal equilibrium averages will be denoted as $\langle \cdots \rangle_T$. We take here the parameters $\tilde{J}_0$ and $\tilde{J}$ as system-size independent constants, because this choice ensures a sensible thermodynamic limit {remember that there are $\frac{1}{2}N(N-1)$ equivalent "bonds" J_{ij} in the Hamiltonian and we wish to have a thermodynamic limit where the energy is an extensive quantity, i.e., $\lim_{N\to\infty}[\langle \mathscr{H} \rangle_T]_{\text{av}}/N$ is finite and in general nonzero}. Analytical work[5-9] usually assumes a Gaussian distribution of bonds,

$$P_G(J_{ij}) = \frac{1}{\sqrt{2\pi}\,(\Delta J)} \exp\left\{-\frac{(J_{ij}-J_0)^2}{2(\Delta J)^2}\right\} \tag{4}$$

Instead of Eq. (4) we use here a bimodal distribution of bonds,

$$P_b(J_{ij}) = x\delta(J_{ij}-J) + (1-x)\,\delta(J_{ij}+J) \tag{5}$$

where the concentration x of ferromagnetic bonds and their strengths J are chosen such that the first two moments yield Eqs. (2), (3) and thus coincide with the moments of the Gaussian distribution,

$$x = \tfrac{1}{2}(1 + J_0/J), \qquad J = \sqrt{J_0^2 + (\Delta J)^2} \tag{6}$$

Since the higher order cumulants of this distribution vanish with higher powers of N^{-1} than Eqs. (2), (3), the results obtained for Eq. (5) will coincide with those of Eq. (4) in the thermodynamic limit. It has even been

shown that the leading terms in finite-size scaling will coincide.[23] Equation (5) is more convenient for numerical calculations and allows faster Monte Carlo simulation codes.

We now choose units such that $\tilde{J}=1$ and Boltzmann's constant $k_B=1$, such that the spin glass transition simply occurs for $T_c=1$. Now it is important to recall that for $\tilde{J}_0<(4-p)/2$ there exists a second transition to a different type of spin glass phase (sometimes called "randomly canted ferromagnetic phase"),[6-8] at a transition temperature T_2 given by

$$T_2=(p/2-1)/(1-\tilde{J}_0) \tag{7}$$

It is clearly advisable not to mix up two different types of phase transitions in a finite-size scaling analysis. Therefore we choose $\tilde{J}_0$ such that T_2 occurs halfway between zero temperature and $T_c=1$, i.e., $T_2=1/2$. With this choice and Eqs. (6), (7) the explicit choices for x and J become

$$x=\frac{1}{2}\left(1+\frac{3-p}{\sqrt{(3-p)^2+N-1}}\right) \tag{8}$$

$$J=\sqrt{(3-p)^2+N-1}/(N-1) \tag{9}$$

For $p=3$ this reduces to the simple result $x=1/2$, $J=1/\sqrt{N-1}$.

For defining the "magnetization" and the glass order parameter for Potts models it is necessary to choose a suitable coordinate system to represent the p states that the spins can take. As usual we choose the simplex representation,[13,28] i.e., the states S_i correspond to $(p-1)$-dimensional unit vectors pointing towards the λth corner of a p-simplex, i.e.,

$$\vec{S}_i^{(\lambda)}\cdot\vec{S}_j^{(\lambda')}=(p\delta_{\lambda\lambda'}-1)/(p-1), \qquad \lambda,\lambda'=1,\ldots,p \tag{10}$$

E.g., for $p=3$ the space of the three vectors $\vec{S}_i^{(1)}$, $\vec{S}_i^{(2)}$, $\vec{S}_i^{(3)}$ representing the values of the Potts spin S_i at site i is two-dimensional and their x, y coordinates are denoted as $\{S_i^\mu\}=(S_i^1, S_i^2)$. The vectors read as follows

$$\vec{S}_i^{(1)}=(0,1), \qquad \vec{S}_i^{(2)}=(\sqrt{3}/2,-1/2), \qquad \vec{S}_i^{(3)}=(-\sqrt{3}/2,-1/2) \tag{11}$$

2.2. Quantities Recorded

In this study we have focused on low order moments of the Hamiltonian, the magnetization and the order parameter. From the moments of the Hamiltonian one straightforwardly gets the internal energy

u per spin, the specific heat c_V per spin and the fourth order energy "cumulant" V_4,

$$E^{(n)} \equiv [\langle \mathscr{H}^n \rangle_T]_{\text{av}}, \qquad u = E^{(1)}/N, \qquad n = 1, 2, 3, 4 \tag{12}$$

$$c_V = [\langle \mathscr{H}^2 \rangle_T - \langle \mathscr{H} \rangle_T^2]_{\text{av}}/(NT^2) \tag{13}$$

$$V_4 \equiv \{3 - E^{(4)}/(E^{(2)})^2\}/2 \tag{14}$$

Note that V_4 sometimes is used as an indicator of "standard" first-order phase transitions in the context of finite-size scaling analyses.[21, 29] Note that $c_V = (\partial u/\partial T)_N$ differs from an analogous quantity c'_V,

$$c'_V = \{E^{(2)} - (E^{(1)})^2\}/(NT^2) \tag{15}$$

due to the lack of self-averaging in systems with quenched disorder.[26, 27]

Now the magnetization $\vec{M}$ is a $(p-1)$-dimensional vector, as noted above, which has $p-1$ components

$$M_\mu = \sum_{i=1}^{N} S_i^\mu, \qquad m = |\vec{m}| \equiv |\vec{M}|/N = \sqrt{\sum_{\mu=1}^{p-1} M_\mu^2}/N \tag{16}$$

The moments of the magnetization per spin then are given as

$$m^{(n)} \equiv [\langle m^n \rangle_T]_{\text{av}} \tag{17}$$

while the "susceptibility" becomes

$$\chi \equiv N[\langle m^2 \rangle_T - \langle m \rangle_T^2]_{\text{av}}/T \tag{18}$$

Again we note that an analogous quantity χ' similar to Eq. (15) can be studied

$$\chi' \equiv N\{m^{(2)} - (m^{(1)})^2\}/T \tag{19}$$

which differs from χ because of the lack of self-averaging. Also a fourth order cumulant $U_4 = (p-1)\{(p+1)/(p-1) - m^{(4)}/(m^{(2)})^2\}/2$ was studied,[30] but the behavior of this quantity is less interesting and hence not considered here.

For defining an order parameter, we follow standard practice[17, 25, 31] to consider two real replicas of the system 1, 2 with identical bond configuration, which evolve independently in parallel in the course of the Monte Carlo simulation. This order parameter hence is a tensorial variable,

$$q^{\mu\nu} = \frac{1}{N} \sum_{i=1}^{N} S_{i,1}^\mu S_{i,2}^\nu, \qquad \mu, \nu = 1, 2, \ldots, p-1 \tag{20}$$

Since in the simulation we only consider the disordered phase of the system where the symmetry is not broken (we also do not use any fields coupling either to components of the order parameter or the magnetization), we again introduce a "root mean square" order parameter in analogy to Eq. (16)[17, 25, 31]

$$q = \sqrt{\sum_{\mu,\nu=1}^{p-1} (q^{\mu\nu})^2} \tag{21}$$

and define moments of the order parameter,

$$q^{(n)} \equiv [\langle q^n \rangle_T]_{\text{av}} \tag{22}$$

Note that the standard spin glass susceptibility is just related to the second moment of the order parameter,[1]

$$\chi_{SG} \equiv N q^{(2)} \tag{23}$$

and it has proven useful[17, 31] to define a fourth-order cumulant g_4

$$g_4 = (p-1)^2 \{1 + 2/(p-1)^2 - q^{(4)}/(q^{(2)})^2\}/2 \tag{24}$$

2.3. A Brief Review of Exact and Phenomenological Results for $N \to \infty$

For $p \leqslant p_c = 4$ there is a second-order transition at $T_c = 1$, and within the replica formalism[1–4] the replica symmetry is not broken for $T \geqslant T_c$. As a consequence, one can model[32] the spin glass transition in terms of a simple Landau-type theory with a scalar order parameter q, writing the free energy density $f(q, m)/k_B T$ as follows

$$f(q, m)/k_B T = \frac{1}{2} r' \left(1 - \frac{T_c}{T}\right) q^2 + \frac{1}{6} u q^3 + \frac{1}{2} r'' m^2 + \cdots \tag{25}$$

where r', u, r'' are coefficients that remain nonzero, positive, and analytic at T_c. Minimizing this free energy density for $T < T_c$ {where Eq. (25) is only qualitatively correct because of broken replica symmetry} would yield a linear vanishing of the order parameter at T_c,

$$q = \frac{2r'}{u}\left(\frac{T_c}{T} - 1\right), \text{ i.e., } q \propto (1 - T/T_c)^{\beta_{SG}} \text{ with } \beta_{SG} = 1 \tag{26}$$

while for $T > T_c$ one concludes that there is a Curie-Weiss like divergence of χ_{SG} while χ remains finite,

$$\chi_{SG} \propto \left[r' \left(1 - \frac{T_c}{T} \right) \right]^{-1}, \text{ i.e., } \chi_{SG} \propto (1 - T/T_c)^{-\gamma_{SG}} \text{ with } \gamma_{SG} = 1 \quad (27)$$

$$\chi \propto r''^{-1} = \text{finite at } T_c \quad (28)$$

Now a phenomenological description of the finite-size scaling limit can be obtained from Eq. (25) by simply taking this expression in the argument of a Boltzmann factor to obtain the probability distribution of $P(q, m)$ in a finite system[25]

$$P(q, m) = \exp[-Nf(q, m)/k_B T] \Big/ \int dq \int dm \exp[-Nf(q, m)/k_B T] \quad (29)$$

or the corresponding reduced distributions {note that to the low order of the Landau expansion considered in Eq. (25), q and m are not coupled, while in higher order terms of order $q^2 m^2$ etc. should appear}

$$P(q) = \int P(q, m)\, dm = \frac{\exp\{-N(\frac{1}{2}r'(1 - T_c/T)\, q^2 + \frac{1}{6}uq^3)\}}{\int dq \exp\{-N(\frac{1}{2}r'(1 - T_c/T)\, q^2 + \frac{1}{6}uq^3)\}} \quad (30)$$

$$P(m) = \int P(q, m)\, dq = \exp(-Nr''m^2/2) \Big/ \int dm \exp(-Nr''m^2/2) \quad (31)$$

Now from Eqs. (30), (31) the leading behavior in the finite-size scaling limit can be inferred qualitatively {a quantitative estimation of prefactors and scaling functions is not possible, since for finite N replica-symmetry breaking must be accounted for even for $T \geqslant T_c$ [23]}. This is simply done by calculating suitable moments,

$$q^{(k)} = \int q^k P(q)\, dq = N^{-k/3} \tilde{f}_k \{N^{1/3}(1 - T_c/T)\} \quad (32)$$

$$m^{(k)} = \int m^k P(m)\, dm = N^{-k/2} \tilde{\tilde{f}}_k (1 - T_c/T) \quad (33)$$

Note that in the considered approximation the argument of the scaling function $\tilde{f}_k$ can simply be understood noting that the argument of the exponential in Eq. (30) can be written as $(N^{1/3}q)^3\, u/6 + (N^{1/3}q)^2\, \{N^{1/3}(1 - T_c/T)\}\, r'/2$, and thus $q^{(k)}$ at T_c must scale like $N^{-k/3}$, and temperature enters in the scaled

combination $N^{1/3}(1-T_c/T)$ only. We thus also conclude for the scaling of the spin glass susceptibility

$$\chi_{SG} = Nq^{(2)} = N^{1/3}\,\tilde{f}_2\{N^{1/3}(1-T_c/T)\} \tag{34}$$

while the ferromagnetic susceptibility should not have any interesting size effects at all,

$$\chi \propto Nm^{(2)} = \tilde{\tilde{f}}_2(1-T_c/T) \tag{35}$$

noting that $\tilde{\tilde{f}}_2$ is a regular function of temperature at T_c {its temperature dependence results only from assuming a temperature dependence of r_2'' in Eq. (25)}.

We emphasize that Eqs. (29)–(34) are rather speculative since replica-symmetry breaking is completely neglected in this argument. However, for the Ising spin glass ($p=2$) Parisi *et al.*[24] basing on an infinite level of replica-symmetry breaking, as is appropriate for this case, derived results compatible with Eqs. (32), (34). Thus it is plausible to assume that Eqs. (32), (34) hold also for the Potts glass for $p>2$, despite the fact that the nature of replica-symmetry breaking (one level is sufficient) differs there from the Ising spin glass.[6, 7]

It is also interesting to note the analogy of the result[25] $q^{(1)} \sim N^{-1/3}$ for the spin glass order parameter at T_c with the results for the percolation probability in infinite range percolation at p_c,[33, 34] $P_\infty(N) \propto N^{-1/3}$. This analogy is not accidental, since considering the $p \to 1$ limit of Potts models one does obtain percolation.[13, 35]

This description, however, cannot even apply qualitatively for $p > p_c = 4$ where a first-order glass transition occurs and q jumps discontinuously from zero to $q_{\text{jump}} > 0$.[6–8] The value of q_{jump} is only known to leading order of a $p-4$ expansion,[7]

$$q_{\text{jump}} = \frac{2(p-4)}{-p^2+18p-42} \qquad \left(=\frac{2}{15} \text{ for } p=6\right) \tag{36}$$

It should also be noted that the distribution of the order parameter $P(q)$ near T_c according to the replica theory[6, 7] is predicted to behave as $P(q) = (1-w)\,\delta(q) + w\delta(q-q_{\text{jump}})$, where the weight w of the peak at $q = q_{\text{jump}}$ vanishes as T_c is approached, $w \propto (1-T/T_c)$. This behavior implies that all moments vanish continuously, $q^{(k)} \propto q^{(k)}_{\text{jump}}(1-T/T_c)$. This behavior is not at all described by the simple free energy ansatz, Eq. (25), and hence the derivation of a phenomenological finite-size scaling description for this case is rather nontrivial. In the appendix some speculative

attempts to formulate such an approach will be discussed, starting, e.g., from the standard theory of finite-size scaling for first-order transitions with non-vanishing latent heat.[21, 29, 36–38]

2.4. Lack of Self-Averaging at Criticality

Wiseman and Domany[26] and Aharony and Harris[27] suggested to consider in random systems the following ratios

$$R_X \equiv [(\langle X \rangle_T - [\langle X \rangle_T]_{\text{av}})^2]_{\text{av}} / [\langle X \rangle_T]^2_{\text{av}} \tag{37}$$

where X are critical quantities (such as magnetization or susceptibility in ferromagnets, etc.). For systems such as short range ferromagnets with random bonds, random fields and random anisotropies it was concluded that[27]

$$R_X \to C_X, \qquad \text{if} \quad L/\xi \to 0 \qquad (\text{i.e., for } T = T_c) \tag{38}$$

$$R_X \propto (\xi/L)^d, \qquad \text{if} \quad L \gg \xi \tag{39}$$

where L is the linear dimension of the d-dimensional system, ξ the order parameter correlation length, and C_X is a universal constant. While Eq. (39) expresses "strong self averaging" (the relative fluctuation vary inversely with the volume[39]), Eq. (38) exhibits lack of self averaging at criticality. On the other hand, considering a quantity Y that is non-critical at T_c (such as the internal energy of the short range system, which is nonzero at T_c) one finds "weak self averaging" (i.e., R_u decays with a smaller power of L than d at T_c).[26]

We now assume that Eqs. (38), (39) can be carried over to systems with long range interactions by using Eqs. (38), (39) for a short range system at the upper critical dimension $d = d_u$, where the hyperscaling relation holds with mean-field exponents, $d_u \nu_{MF} = \gamma_{MF} + 2\beta_{MF}$, and using $L^{d_u} = N$ we conclude for random mean-field ferromagnets

$$R_X \to C_X, \qquad T = T_c, \qquad N \to \infty \tag{40}$$

$$R_X \propto 1/[(1 - T_c/T)^{2\beta_{MF} + \gamma_{MF}} N], \qquad N \gg (1 - T_c/T)^{-(2\beta_{MF} + \gamma_{MF})} \tag{41}$$

If we make the further assumption that Eqs. (40), (41) are not only true for the random ferromagnets considered in refs. 26 and 27, but for spin glass systems as well where $d_u = 6$, $\nu_{MF} = 1/2$, $\beta_{MF} = 1$, $\gamma_{MF} = 1$, we conclude that Eq. (41) can be written as

$$R_X \propto 1/[N(1 - T_c/T)^3] \qquad \text{if} \quad N(1 - T/T_c)^3 \gg 1 \tag{42}$$

We thus find that in general the ratio R_X has a scaling structure analogous to Eq. (32),

$$R_X = C_X \tilde{R}\{N^{1/3}(1 - T_c/T)\} \tag{43}$$

with $\tilde{R}(z \gg 1) \propto z^{-3}$. We expect this behavior in our case hence for the moments of the order parameter distribution, i.e., for $X = q^n$, with $n = 1, 2, \ldots$. On the other hand, if self-averaging holds for quantities such as energy and magnetization, which are non-critical quantities in our case, we expect that the ratios

$$R_u \equiv [(\langle \mathscr{H} \rangle_T - [\langle \mathscr{H} \rangle_T]_{\text{av}})^2]_{\text{av}} / [\langle \mathscr{H} \rangle_T]^2_{\text{av}} \tag{44}$$

$$R_{m^n} \equiv [(\langle m^n \rangle_T - [\langle m^n \rangle_T]_{\text{av}})^2]_{\text{av}} / [\langle m^n \rangle_T]^2_{\text{av}}, \qquad n = 1, 2, \ldots \tag{45}$$

vanish even at T_c for large N,

$$\lim_{N \to \infty} R_u(T = T_c) = 0, \qquad \lim_{N \to \infty} R_{m^n}(T = T_c) = 0 \tag{46}$$

For finite N these ratios R_u, R_{m^n} clearly are nonzero, but we do not know an argument to predict the power laws with which these ratios should vanish as $N \to \infty$. In any case Eq. (46) has the consequence that the quantities c_V, c'_V converge for $N \to \infty$ to the same limit, as well as that χ, χ' converge to the same limit, which one can derive using Eq. (46) straightforwardly in the definitions Eqs. (13), (15) or Eqs. (18), (19), respectively.

2.5. Monte Carlo Procedures

Standard Metropolis Monte Carlo simulations have been carried out, putting most effort on $T = T_c = 1$, but considering for $p = 3$ also a range of temperatures below T_c (usually $0.98 \leqslant T \leqslant 1.0$), in order to be able to locate the temperatures $T_{\max}(N)$ of the specific-heat maxima, which fall into this region. For $p = 6$, on the other hand, data for considerably higher temperatures than $T_c = 1$ were necessary (up to $T = 2$–3 for $N = 5$) to be able to locate the specific-heat maximum. For being able to locate the specific-heat maxima, we have used the exact calculations of ref. 25 as guidance for the temperature range where the maximum should occur, and then recorded typically 3–5 temperatures in that region, which where used as a starting point for an interpolation with standard multihistogram methods[40] to generate smooth curves that "connect" the original data points. This needs to be done independently for each sample of bond

configurations. The sample averaging (using in practice a sample of 200 configurations) then is done as a last step. Because of the large storage requirements, such a reweighting was done only for the energy distribution (allowing thus to calculate internal energy, specific heat etc. over some temperature range), but not for the joint distribution of energy and order parameter, which would be needed to obtain reweighted order parameter moments as well. Most effort hence was devoted to obtain the various quantities right at T_c. Since $T_c = 1$ is known in the present model beforehand the calculation this allows the most stringent tests of the theoretical concepts anyway.

Since the model is believed to exhibit a "dynamical phase transition"[14, 15] at some temperature $T_D > T_c$, however, critical slowing down could be a serious problem for our approach, hampering the accuracy that can be reached. Of course, for small N we do expect that also all divergencies of relaxation time are rounded off, irrespective whether they occur at T_D or T_c. Nevertheless it is important to assess the accuracy, that is actually reached, since it is known that the statistical error of a quantity A is enhanced by a factor $2\tau_A$ relative to the error that would be obtained for statistically independent data,[41–43]

$$(\delta A)^2 = \frac{2\tau_A}{\mathcal{N}} [\langle A^2 \rangle - \langle A \rangle^2] \tag{47}$$

where $\mathcal{N}$ is the number of observations used for computing the averages. Here τ_A is interpreted as the integrated autocorrelation time of the quantity A, and Eq. (47) is valid if τ_A is much larger than the time between the successive "measurements" used to compute the averages.[41–43]

As a crude method to both estimate roughly this autocorrelation time τ_A and the actual statistical errors, we have analyzed for some examples the time series for various data by a binning method. I.e., the $\mathcal{N}$ observations are combined into $\mathcal{N}/b$ blocks of size b, carrying out a sub-average of A ($\bar{A}_l$) over every block (labeled by an index l). Then an error is calculated as ($\tilde{\mathcal{N}} = \mathcal{N}/b$)

$$\Delta A(b) = \left\{ \frac{1}{\tilde{\mathcal{N}}(\tilde{\mathcal{N}} - 1)} \sum_{l=1}^{\tilde{\mathcal{N}}} (\bar{A}_l - \bar{A})^2 \right\}^{1/2}, \qquad \bar{A} = \frac{1}{\tilde{\mathcal{N}}} \sum_{l=1}^{\tilde{\mathcal{N}}} \bar{A}_l \tag{48}$$

Only if b exceeds $\approx 2\tau_A$, will $\Delta A(b)$ settle down at the correct error estimate, which does not depend on b systematically, while if $b < 2\tau_A$ the error is systematically too small, but increases with increasing b.

Figure 1 shows two typical examples where this method was used for the energy per spin. One can see that for $T = 1$ and $N = 60$ the autocorrelation

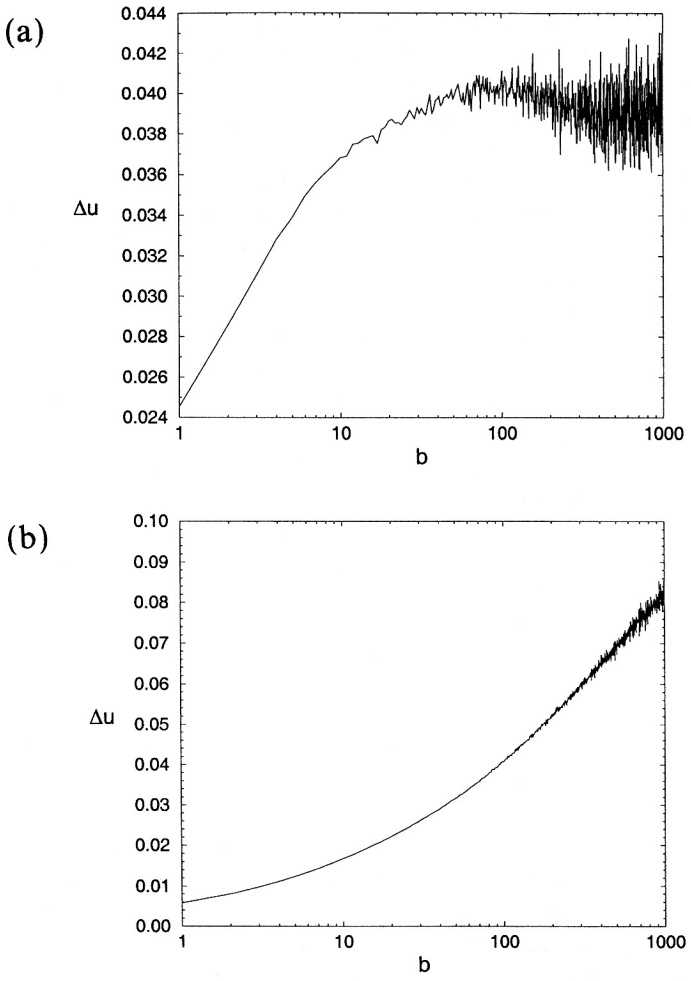

Fig. 1. Error $\Delta u(b)$ of the energy per spin plotted versus the bin size for the case $p=6$, $T=1$, $N=60$, taking measurements every 10 MCS/spin (a) and for the case $p=6$, $T=0.5$, $N=30$, with measurements taken in every update step (b).

time is still rather small ($\tau_u \approx 13$ in units of MCS/spin for $p=6$) while for $T=0.5$ even small systems (such as $N=30$) do not converge to a plateau during a reasonable autocorrelation time (which is at least $\tau_u = 250$ in the example shown in Fig. 1 but possibly much larger). Therefore no attempt could be made to study the lower transition at $T_2 = 0.5$.

Another crucial observation that our procedures for equilibration and averaging are sufficient {typically averages were taken over 500000

MCS/spin for each sample, taking observations every 100 MCS/spin, and before the averaging begins a comparably large run is made with no averages taken to properly equilibrate the data} is the very good agreement with the exact calculations of ref. 25, of course. This fact will become apparent in the following sections.

Particular care is necessary[26] in estimating the ratios R_X {Eq. (37)}, since the Monte Carlo simulation does not yield $\langle X \rangle_T$ exactly but only an average $\bar{X}$ which differs from $\langle X \rangle_T$ by some statistical error δX, with $[\delta X]_{\text{av}} = 0$ but $[(\delta X)^2]_{\text{av}} \neq 0$. If one hence estimates R_X by $\bar{R}_X$ defined by

$$\begin{aligned} \bar{R}_X &= [(\bar{X} - [\bar{X}]_{\text{av}})^2]_{\text{av}} / [\bar{X}]_{\text{av}}^2 \\ &= \{[(\langle X \rangle_T - [\langle X \rangle_T]_{\text{av}})^2] + [(\delta X)^2]_{\text{av}}\} / [\langle X \rangle_T]_{\text{av}}^2 \end{aligned} \tag{49}$$

one would systematically overestimate the true R_X. Although in our case at T_c the contribution due to $[(\delta X)^2]_{\text{av}}$ always was relatively small, we have corrected for it, as suggested by Wiseman and Domany.[26]

3. NUMERICAL RESULTS FOR THE $p = 3$ STATE POTTS GLASS

We start our discussion by presenting the temperature dependence of the second moment of the order parameter $q^{(2)}$ for small systems ($N \leqslant 15$), where "exact" results[25] are available (Fig. 2). It is seen that there is excellent agreement over the full temperature range (for such small N as

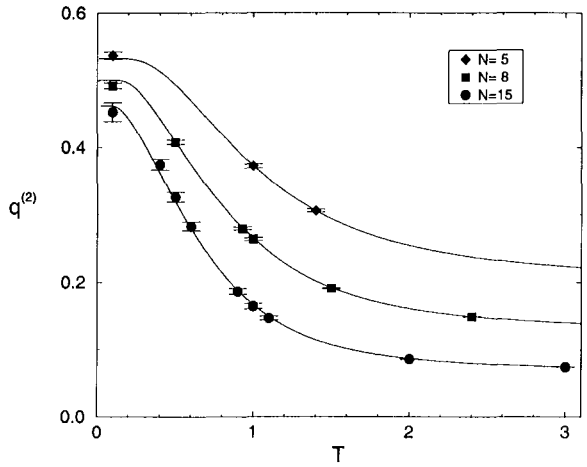

Fig. 2. Second moment of the order parameter distribution of the 3-state Potts glass $q^{(2)}$ plotted vs. temperature T for $N = 5$, 8 and 15. Symbols with error bars are the present Monte Carlo results, while curves represent the "exact" calculations of Peters *et al.*[25]

shown in Fig. 2 the growth of the relaxation times at and below T_c is so strongly rounded that one can perform the Monte Carlo simulations also at low temperatures). Ref. 30 contains many more such comparisons which all show similar agreement (including the case $p=6$) and thus establish that the accuracy of our Monte Carlo procedures is well under control.

Figure 3 shows the second and fourth moment of $q^{(2)}$ plotted vs. N^{-1} at $T=T_c=1$. As a first step to analyze the data, they were fitted to equations $y=a+bx^c$, which yielded for $q^{(2)}$ the constants a, b, c as (errors being shown in parenthesis) $a=0.002(2)$, $b=1.169(40)$, $c=0.726(17)$, with a quality Q of the fit $Q=0.93$ and $\chi^2/f=0.435$ (f being the number of degrees of freedom of the fit). For $q^{(4)}$ the analogous numbers are $a=0.3(1.5)\cdot 10^{-4}$, $b=1.614(93)$, $c=2.379(21)$ and $Q=0.835$, $\chi^2/f=0.576$, and for $q^{(1)}$ (not shown here) $a=0.021(11)$, $b=1.041(14)$, $c=0.387(16)$, $Q=0.93$ and $\chi^2/f=0.436$. From these fits one hence can conclude that $a=0$ in all cases, i.e., there is no nonzero order parameter present at T_c for $p=3$, in this respect the Monte Carlo data yield the same conclusion as the replica treatment.[5–8] However, the exponents c resulting from the fits quoted above are not in agreement with the prediction $q^{(k)} \propto N^{-k/3}$ {Eq. (32)}. It is very likely that this deviation results from corrections to finite size scaling. In fact, for the infinite range Ising spin glass one can show from replica symmetry breaking methods the following structure[23, 24]

$$q^{(k)} = C_{(k)} N^{-k/3} + C'_{(k)} N^{-(k+1)/3} + C''_{(k)} N^{-(k+2)/3} + \cdots, \qquad T=T_c \quad (50)$$

It is probable (but remains to be proven) that Eq. (50) holds for the $p=3$ infinite range Potts glass as well. In fact, fits of our data to Eq. (50) are possible, and one obtains "reasonable" values of the coefficients $C_{(k)}$, $C'_{(k)}$ and $C''_{(k)}$ (i.e., the coefficients are of order unity, and the quality of the fits is comparable to the fits quoted above). However, in order to test for the leading power law in a way unbiased by theoretical prejudices, we also proceeded in a different manner, fitting the data from $N=N_{\min}$ up to $N_{\max}=120$ to a simple power law with a free exponent, $y=bx^c$ (with $x=1/N$ as before), varying $N_{\min}$ to see if for large enough $N_{\min}$ the results for the exponent c get stable. In this way, one finds that c decreases systematically with $N_{\min}$ up to about $N_{\min}=30$, while for larger $N_{\min}$ the systematic trend is clearly very small, distinctly smaller than the error of the fit resulting from the statistical errors of the data. Choosing hence $N_{\min}=30$ for all $q^{(k)}$, one finds for the exponent $c=0.347(7)$, $c=0.688(15)$ and $c=1.352(34)$ for $k=1, 2, 4$, respectively. While the predicted exponents $k/3$ are still slightly outside of the error margins of these fits, we do not consider these slight deviations as significant, they can very likely be attributed to a residual effect of the correction terms of Eq. (50) that

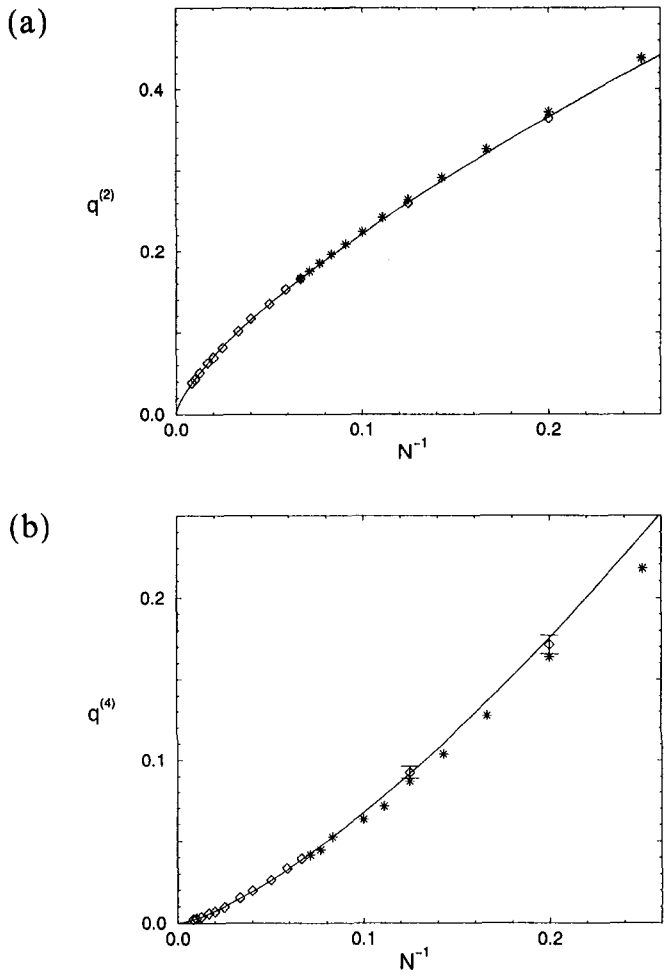

Fig. 3. Second moment $q^{(2)}$ (a) and fourth moment $q^{(4)}$ (b) of the order parameter distribution for $p=3$ at $T=T_c=1$ plotted vs. N^{-1}. Asteriks represent "exact" data from Peters *et al.*,[25] diamonds show the present Monte Carlo results. Error bars are only shown if they exceed the size of the symbols. Curves are fits through the data points as mentioned in the text.

still influence the data for $N \geqslant N_{\min}=30$ a little. As a corollary of this conclusion, Fig. 4 shows plots of $q^{(2)}$ and $q^{(4)}$ vs. $N^{-2/3}$ and $N^{-4/3}$, to demonstrate also by visual inspection that for large enough N the scaling relation $q^{(k)} \propto N^{-k/3}$ holds. The straight lines shown in Fig. 4 are fits to $y=a+bx$ with parameters $a=-0.002(1)$, $b=0.981(23)$, $\chi^2/f=0.700$ and

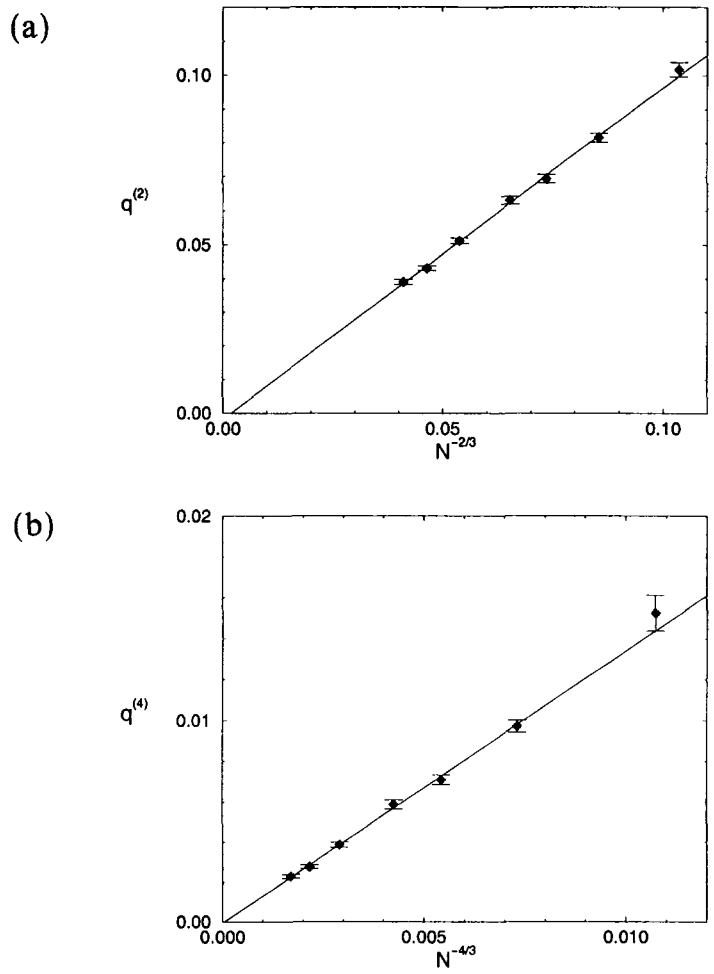

Fig. 4. Second moment $q^{(2)}$ (a) and fourth moment $q^{(4)}$ (b) of the order parameter distribution for $p=3$ at $T=T_c=1$ plotted vs. $N^{-2/3}$ (a) or $N^{-4/3}$ (b), including only data for $N \geqslant N_{\min}=30$.

$Q=0.623$ in case (a), and $a=-0.5(1.2)\cdot 10^{-4}$, $b=1.346(40)$, $\chi^2/f=0.711$ and $Q=0.615$ in case (b).

Having tested the scaling of $q^{(k)} \propto N^{-k/3}$ for $T=T_c$, it also is of interest to check to what extent our data are compatible with the full scaling structure of Eq. (32) considering off-critical temperatures. Figure 5 shows scaling plots for the first two moments, including even the smallest values of N studied. Although there is some statistical scatter and also systematic

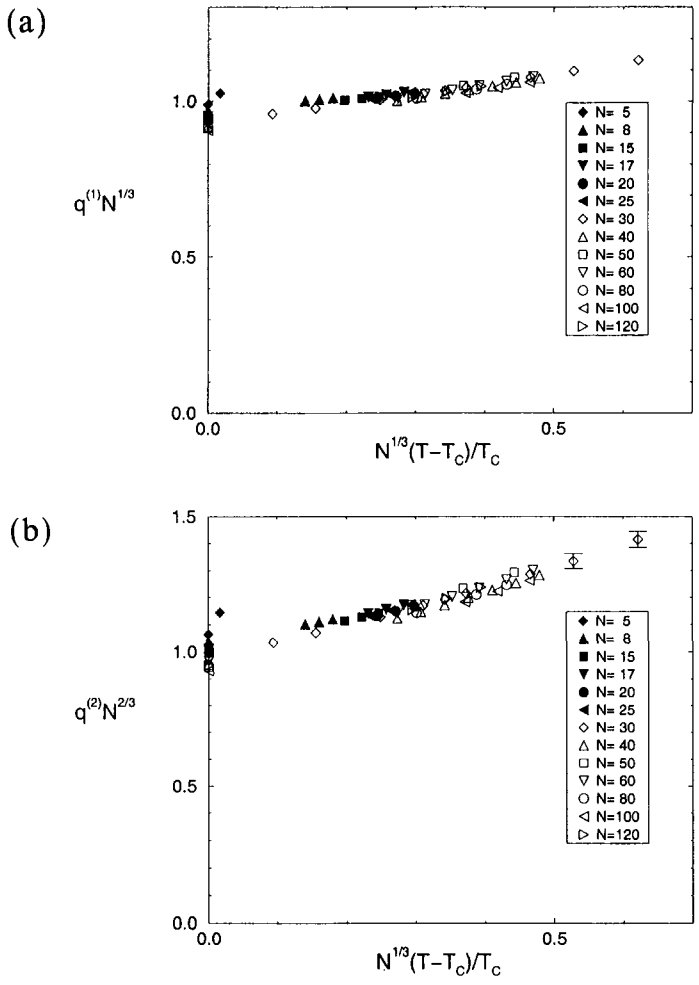

Fig. 5. Plot of $q^{(1)}N^{-1/3}$ (a) and $q^{(2)}N^{-2/3}$ (b) vs. the scaling variable $N^{-1/3}(T-T_c)/T_c$ for $p=3$. Different symbols show the various values of N, as indicated.

deviations are clearly present (due to the use of too small N and of temperatures too distant from T_c), we do feel that the present data indicate that Eq. (32) is in fact valid, in the appropriate limit where $N\to\infty$ and $T\to T_c$.

Next we are concerned with the magnetization at the critical temperature (Figs. 6 and 7). All moments recorded $\{m^{(1)}, m^{(2)}$ and $m^{(4)}\}$ are in excellent agreement with the "exact" calculations of Peters *et al.*[25] for the corresponding sizes. There is also no doubt that all moments $m^{(k)}$

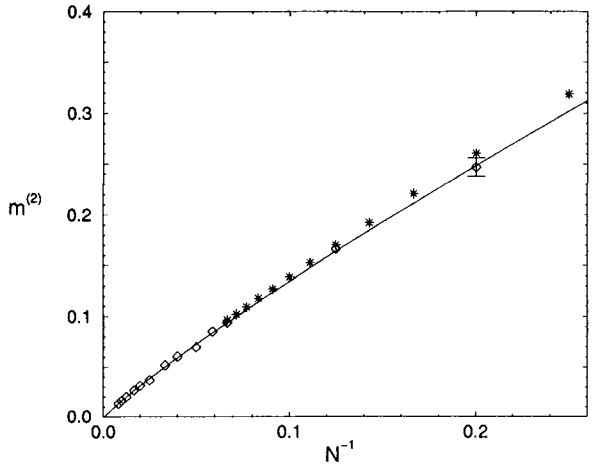

Fig. 6. Plot of the second moment of the magnetization $m^{(2)}$ at T_c as function of N^{-1} for $p=3$. Asteriks represent the "exact" data from Peters *et al.*,[25] diamonds show the present Monte Carlo results. Error bars are only shown if they exceed the size of the symbols. Curve is a fit through the data points of the form $y=a+bx^c$ with $a=-0.002(1)$, $b=1.021(64)$, $c=0.874(26)$, $Q=0.854$ and $\chi^2/f=0.552$.

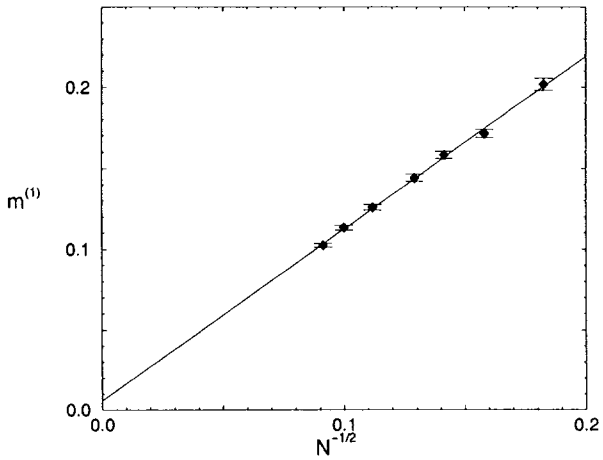

Fig. 7. First moment $m^{(1)}$ of the magnetization distribution at $T=T_c$ plotted vs. $N^{-1/2}$ for $p=3$. Only Monte Carlo data for the 7 largest sizes are shown. Straight line $y=a+bx$ is a result of a fit, with parameters $a=0.006(3)$, $b=1.066(27)$, goodness $Q=0.640$ and $\chi^2/f=0.678$.

vanish as $N \to \infty$. As seen in Fig. 6, one does not really reproduce the expected power laws $m^{(k)} \propto N^{-k/2}$ if one includes all values of N in a fit, due to corrections to the asymptotic behavior. But it is plausible from Fig. 6 that the data for large enough N ($N \geqslant N_{\min} = 30$) are in fact compatible with a straight line through the origin, and this expectation is confirmed by a corresponding fit. The same is true for other moments (Fig. 7). We have also recorded the magnetization at off-critical temperatures, but since it always is rather small and with a sample of $n = 200$ bond configurations the relative error of this sampling ($\sqrt{2/n} = 0.1$) is rather large, a convincing demonstration of the temperature dependence suggested by Eq. (33) has not been attempted.

For the internal energy $u_c = E^{(1)}(T = T_c)/N$ at the critical temperature Parisi *et al.*[23, 24] derived in the case of the Ising infinite range model the finite-size behavior as

$$u_c = u_c^{\infty} + u_c' N^{-2/3} + u_c'' N^{-1} + \cdots \tag{51}$$

Note that this is of the same type as the second moment $q^{(2)}$, as expected, the only distinction being that the limiting value u_c^{∞} is nonzero. Assuming that Eq. (51) also holds for the $p = 3$ Potts glass, we have fitted our data for u_c to Eq. (51) as well. It turns out that restricting the fit to $N \geqslant 15$ the correction term $u_c'' N^{-1}$ can be omitted (Fig. 8).

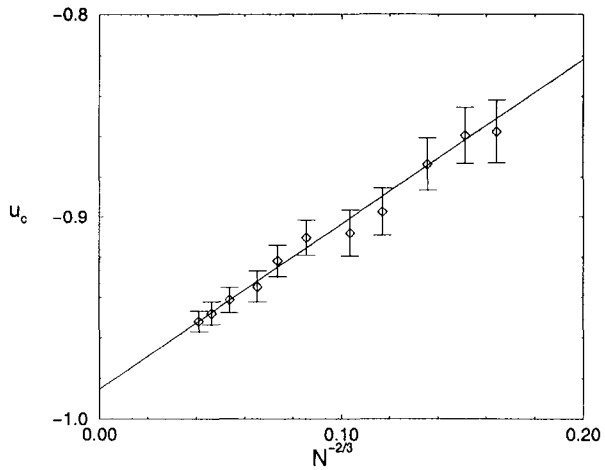

Fig. 8. Internal energy u_c per spin at $T = T_c$ plotted vs. $N^{-2/3}$ for $p = 3$. Straight line $y = a + bx$ shows results from a fit that yielded the parameters $a = -0.985(9)$, $b = 0.818(148)$, with quality $Q = 0.961$ and $\chi^2/f = 0.205$.

A rather interesting behavior is exhibited by the specific heat which shows a maximum $c_V^{\max}$ at a temperature $T_{\max}$ that approaches T_c in a non-monotonic fashion (Fig. 9). One can fit a quadratic parabola to the curve $T_{\max}$ vs. $N^{-1/3}$, as indicated in Fig. 9(b), but it is clear that this does not yield a particularly accurate estimate of T_c if one assumes $T_c = T_{\max}$

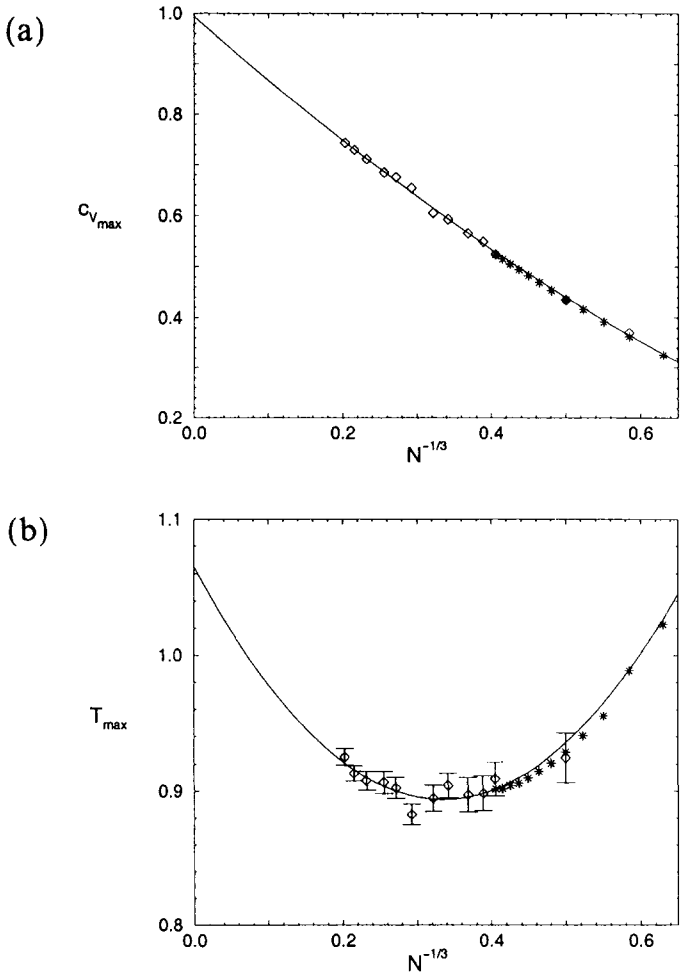

Fig. 9. (a) Maximum of the specific heat $c_V^{\max}$ plotted vs. $N^{-1/3}$ for $p = 3$. Stars represent "exact" data from Peters *et al.*,[25] diamonds show the present Monte Carlo results. Curve is a fit to the equation $y = a + bx^{1/3} + cx^{2/3}$ (with $x = 1/N$) and parameters $a = 0.994(15)$, $b = -1.307(93)$, $c = 0.397(128)$, and quality $Q = 0.408$, $\chi^2/f = 1.037$. (b) $T_{\max}$ plotted vs. $N^{-1/3}$.

$(N \to \infty)$. Both $c_V^{\max}$ (Fig. 9(a)) and $c_V^c = c_V(T = T_c)$ are compatible with a behavior $c_V = c_V^{\text{crit}} + c'_V N^{-1/3} + c''_V N^{-2/3}$.

Finally we return to the ratios R_X characterizing the self-averaging properties {Section 2.4}. Figure 10 shows log-log plots of R_{q^1} and R_{q^2} at $T = T_c$ versus N. If one excludes the smallest sizes $N = 5$, $N = 8$, no systematic N-dependence can be seen, and hence these data are in fact compatible with the lack of self-averaging predicted in Eq. (40).

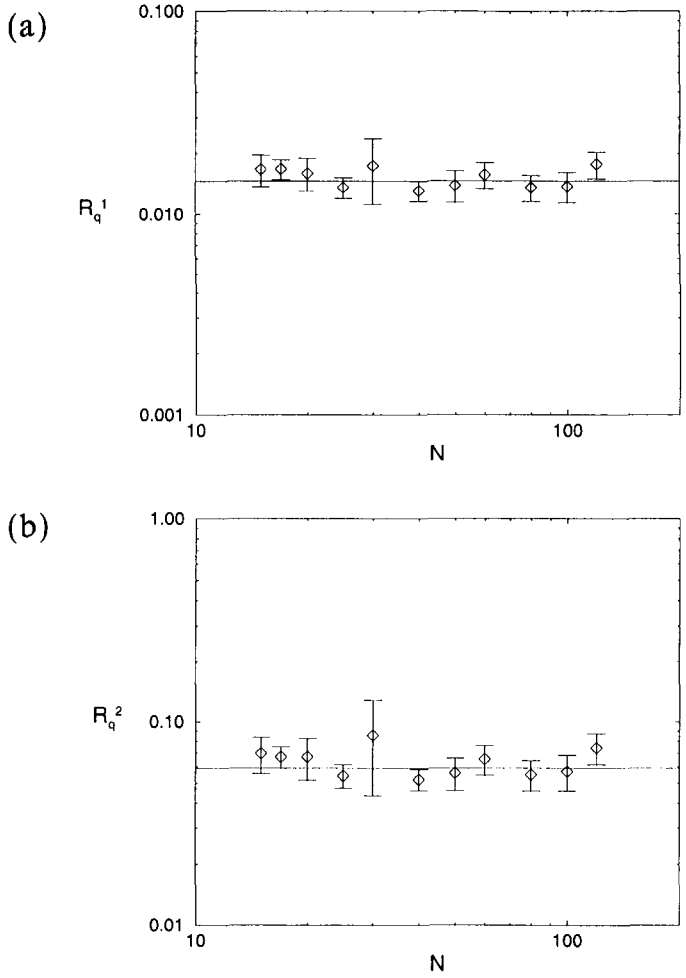

Fig. 10. Log-log plot of ratios R_{q^1} (a) and R_{q^2} (b) for $T = T_c$ versus N for $p = 3$. The horizontal straight lines indicate that the data are compatible with the approach to an N-independent limit.

In contrast, quantities such as u and c_V that reach finite limits u_c and c_V^c at T_c are compatible with strong self-averaging even at T_c (Fig. 11). But the moments of the magnetization, which is a "non-ordering field" at this transition but has moments which vanish only for $N \to \infty$, seems to show weak self-averaging only (Fig. 12). In fact, it seems possible that both R_{m^1} and R_{m^2} show a scaling behavior $R_{m^k} \propto N^{-1/3}$ independent of the order of the moment k. Remembering that the moments of the magnetization did

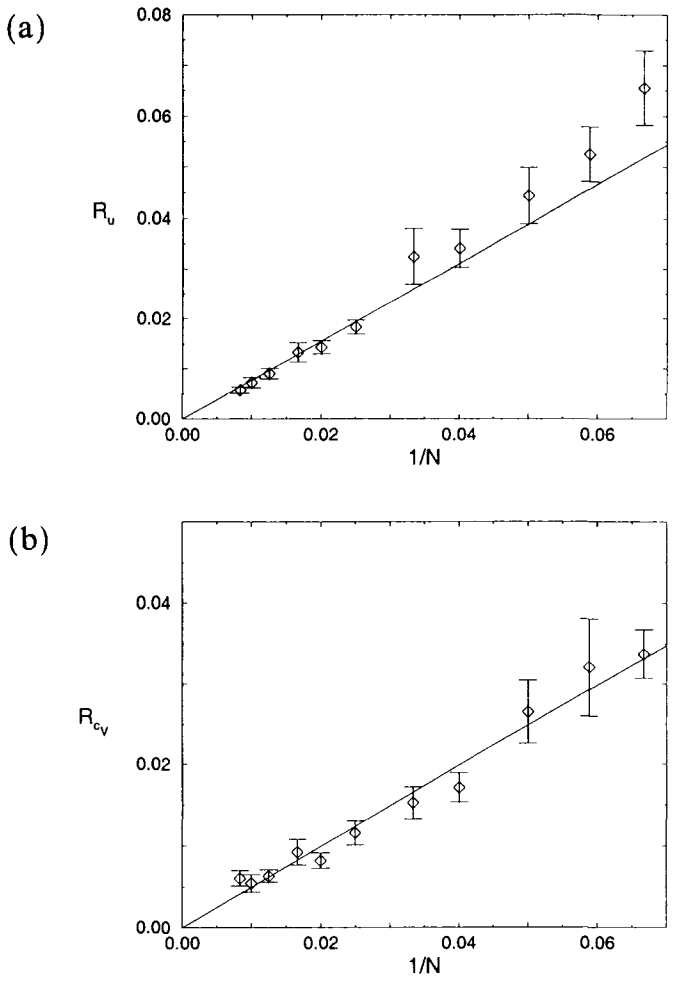

Fig. 11. Plot of the ratio R_u (a) and R_{c_1} (b) at $T = T_c$ versus $1/N$ for $p = 3$.

not scale as powers of $N^{-1/3}$ but rather as powers of $N^{-1/2}$ {Eq. 33, Figs. 6 and 7}, this is somewhat unexpected. Of course, it always is possible that in the regime of N studied the asymptotic size dependence has not been fully reached, and in view of the very large error bars in Fig. 12 any systematic correction to scaling could easily be overlooked. This problem deserves further investigation but would require a substantially larger computational effort than is possible at present.

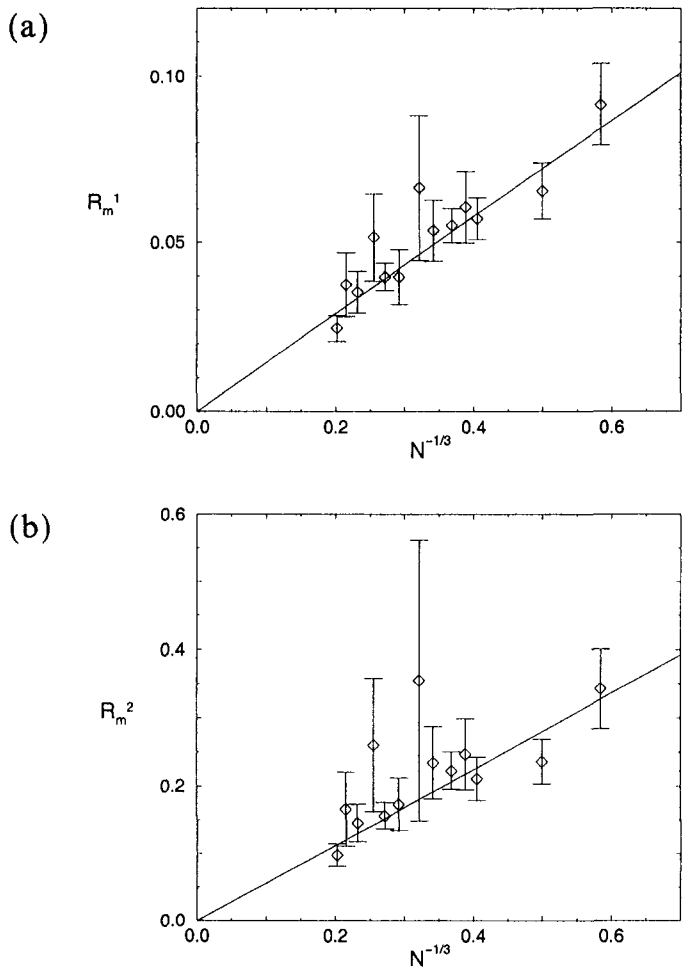

Fig. 12. Plot of the ratios R_{m^1} (a) and R_{m^2} (b) at $T = T_c$ versus $N^{-1/3}$ for $p = 3$.

4. NUMERICAL RESULTS FOR THE $p=6$ STATE POTTS GLASS

Again we start our discussion by focusing on the moments of the order parameter distribution (Figs. 13, 14). As for the case $p=3$, we want to proceed with our analysis in an unbiased fashion, and thus first try fits to the form $y=a+bx^c$ ($x=1/N$) but since we expect that only data for large N can show the asymptotic behavior, we restrict the range of the fit to

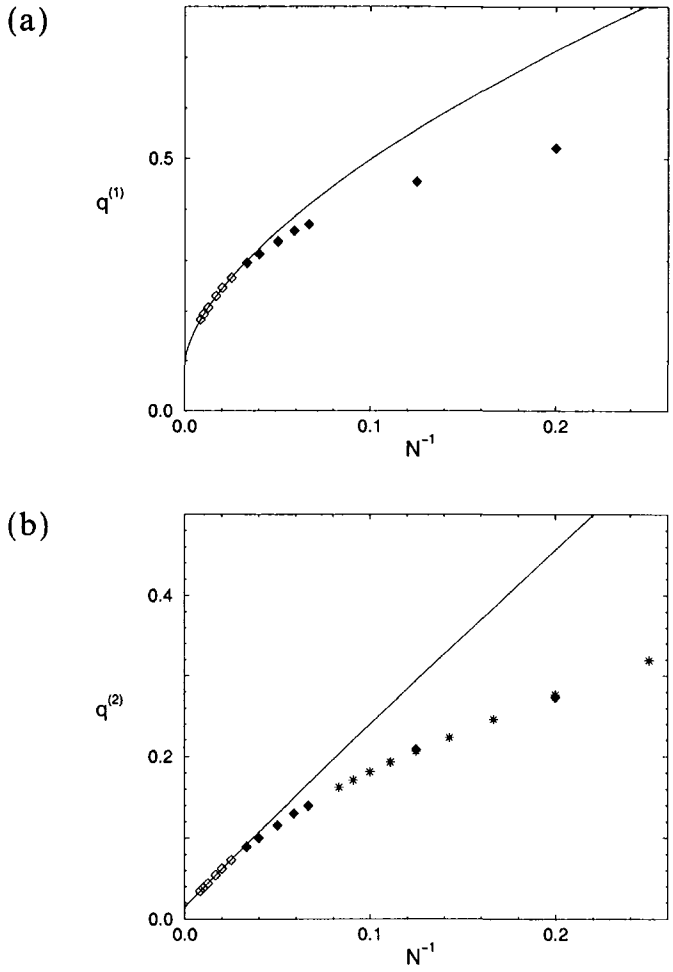

Fig. 13. First moment $q^{(1)}$ (a) and second moment $q^{(2)}$ (b) of the order parameter distribution of the 6-state Potts glass at $T=T_c=1$ plotted vs. N^{-1}. Asteriks denote the "exact" data of Peters *et al.*,[25] while diamonds denote the Monte Carlo data. Only open symbols have been used for fitting the curves shown, which are discussed in the main text.

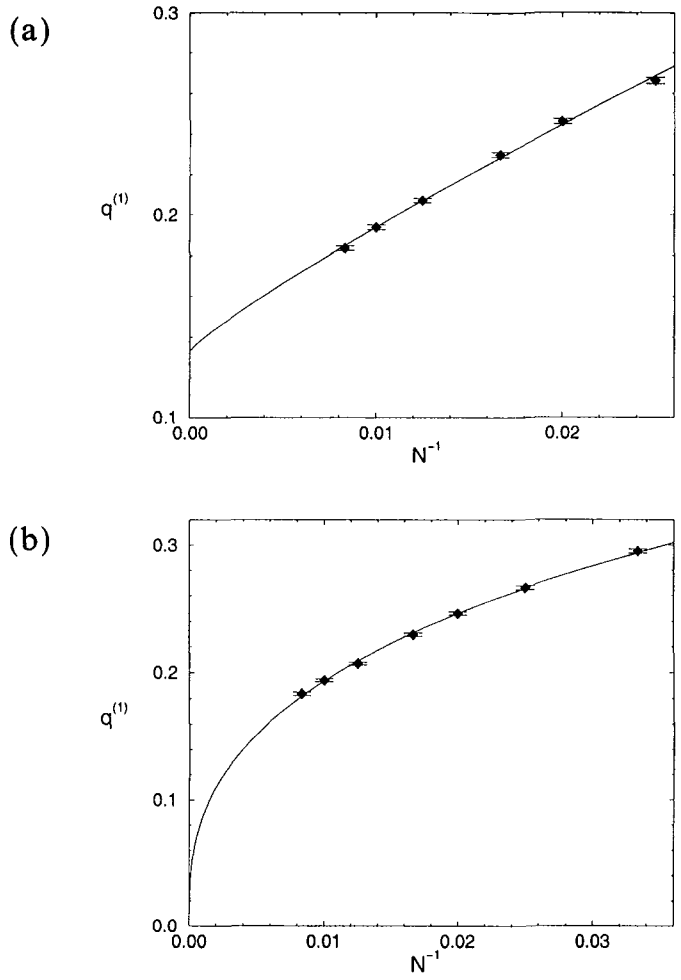

Fig. 14. First moment $q^{(1)}$ plotted vs. N^{-1} as in Fig. 13, but (a) including data only for $N \geqslant N_{\min} = 40$. The curve shown is a fit to the equation $y = 2/15 + bx^c$ with $x = 1/N$, $b = 3.434(232)$ and $c = 0.877(17)$, (b) including data only for $N \geqslant N_{\min} = 30$. The curve shown is a fit to the equation $y = bx^c$ with $x = 1/N$, $b = 0.960(18)$ and $c = 0.348(5)$.

$N \geqslant N_{\min} = 40$ in this section. For $q^{(1)}$, we thus obtain fitted parameters $a = 0.098(23)$, $b = 1.670(510)$, $c = 0.621(118)$, and the quality of the fit is characterized by $\chi^2/f = 0.542$, $Q = 0.653$, while for $q^{(2)}$ the analogous numbers are $a = 0.015(4)$, $b = 2.112(817)$, $c = 0.973(122)$, $\chi^2/f = 0.519$ and $Q = 0.669$. Of course, again the effect of varying $N_{\min}$ was studied, and since the uncertainties of the fit strongly increase with increasing $N_{\min}$, this

value of $N_{\min}$ was again chosen where the systematic trend (e.g., the intercept a systematically increases with increasing $N_{\min}$ but stabilizes for $N_{\min} \geq 40$) gets lost in the uncertainty found from the fit.

The result of these fits for all three moments $q^{(1)}$, $q^{(2)}$ and $q^{(4)}$ hence is that the limiting value for $N \to \infty$ (namely the above constant a) is slightly different from zero. In order to test whether this is a consequence of the first-order transition described by Eq. (36), we have tried a second fit, where $a = (q_{\text{jump}})^k$ with $q_{\text{jump}} = 2/15$ was used as a constraint (Fig. 14(a)). It is seen that such fits are nicely possible also (fits for $q^{(2)}$ and $q^{(4)}$ are of similar quality[30]). However, as mentioned above, such a behavior is not consistent with the replica theory, which rather requires nonzero intercepts for $T < T_c$ only ($a \propto q_{\text{jump}}^k (1 - T/T_c)$). Thus we have also tried a third fit where we impose the constraint $a = 0$ in the fit, $q^{(k)} = bx^c$, Fig. 14(b). Also in this case an acceptable quality of the fit is obtained, and the exponent c for $k = 1$, 2 and 4 is roughly compatible with a behavior $c = k/3$.

While on the basis of their exact enumeration data (included as asteriks in Fig. 13(b)) Peters *et al.*[25] had concluded that $\lim_{N \to \infty} q^{(k)} > 0$, the downturn of the data for $N^{-1} < 0.1$ in Fig. 13(b) already raises some doubt on the firmness of this conclusions, and the comparison of the fits Fig. 14(a), (b) shows that in fact no firm conclusion can be drawn!

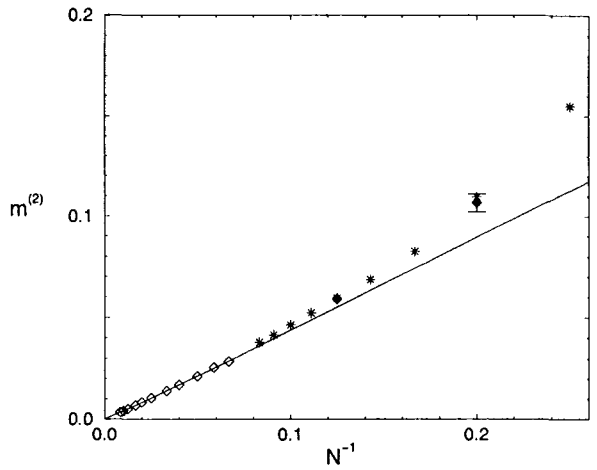

Fig. 15. Second moment of the magnetization distribution $m^{(2)}$ of the 6-state Potts glass at T_c plotted vs. N^{-1}. Asteriks show "exact" data of Peters *et al.*,[25] diamonds show the present Monte Carlo results. Curve is a fit of the function $y = a + bx^c$ ($x = 1/N$) through the data with the open symbols, yielding parameters $a = 2(2) \cdot 10^{-4}$, $b = 0.474(34)$, $c = 1.037(25)$, the quality of the fit being characterized by $\chi^2/f = 0.489$, $Q = 0.865$.

Also for $p=6$ the magnetization is still nicely compatible with the expectation that $m^{(k)} \propto N^{-k/2}$, Eq. (33). Also for first-order glass transitions, the magnetization is decoupled from the order parameter to leading order, and we can assume that Eq. (31) is still valid. Figure 15 shows, as an example (more details are found in ref. 30) a plot of $m^{(2)}$ vs. N^{-1}, demonstrating that the asymptotic regime of the linear behavior is much wider than for the order parameter.

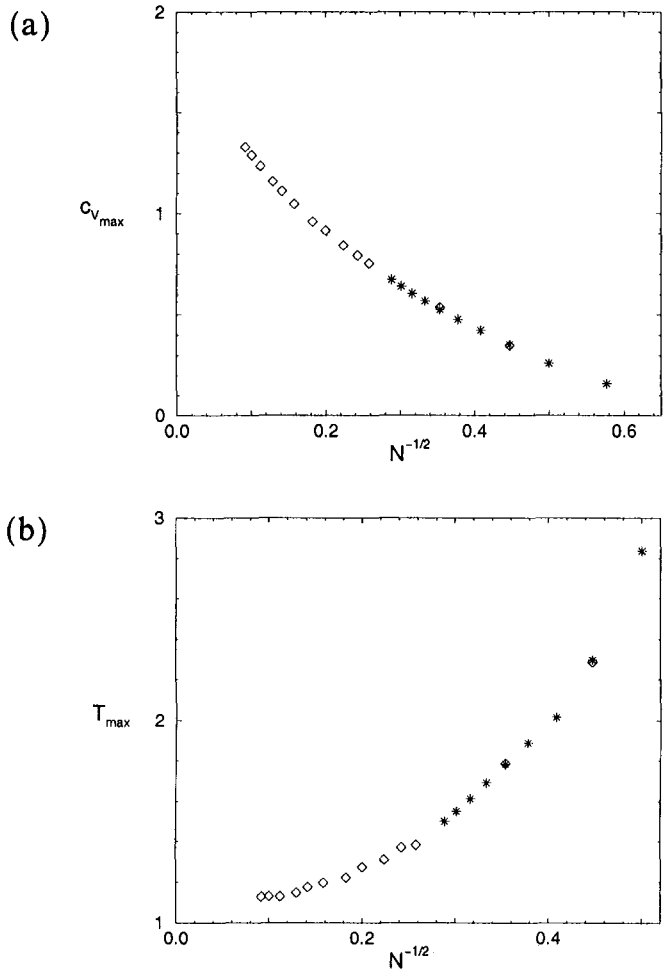

Fig. 16. (a) Maximum c_V^{max} of the specific heat of the 6-state Potts glass plotted vs. $N^{-1/2}$. Asteriks denote the "exact" data of Peters *et al.*,[25] diamonds the present Monte Carlo results. (b) T_{max} plotted vs. $N^{-1/2}$.

Again the behavior of the specific-heat maxima is rather interesting. In view of the phenomenological finite-size scaling theory of the Appendix, which predicts asymptotic variations proportional to $N^{-1/2}$, we have plotted our data against this variable (Fig. 16). Again the agreement with the "exact" data of Peters *et al.*[25] is gratifying, as well as the clear hint that there is no divergence of $c_V^{\max}$ as $N \to \infty$ and hence no latent heat, despite the fact that we have a jump of the glass order parameter at the transition. While the curve $T_{\max}$ vs. $N^{-1/2}$ is very much curved—if the finite-size

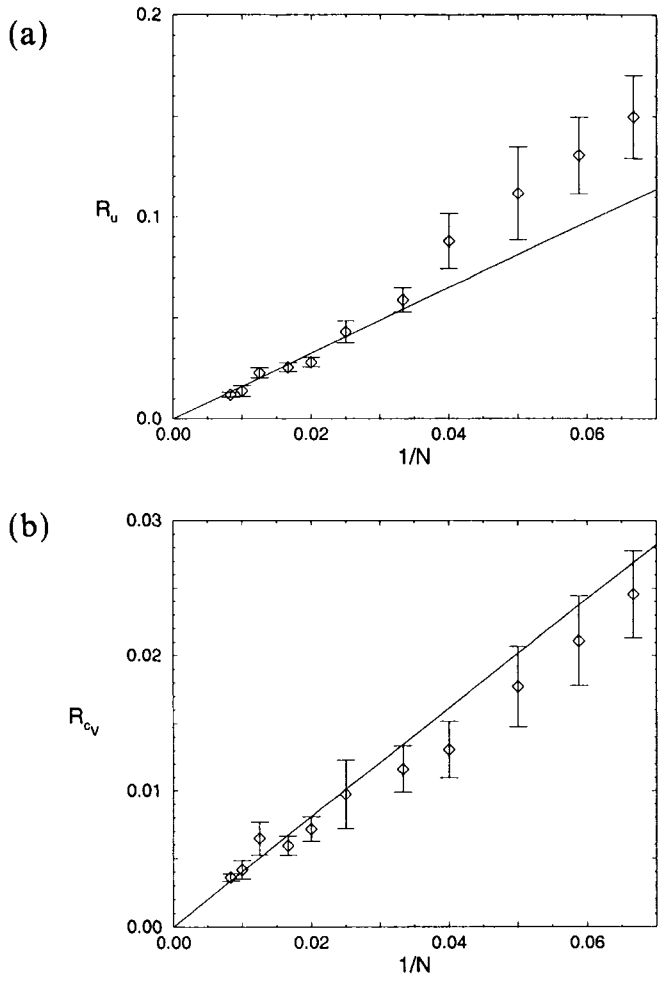

Fig. 17. Plot of the ratio R_u (a) and R_{c_V} (b) at $T = T_c$ versus $1/N$ for $p = 6$.

scaling theory of the Appendix is correct at all, at least doubts could be raised whether any of our data fall in the asymptotic regime of finite-size scaling. Neither for $p = 3$ nor for $p = 6$ extrapolation of specific-heat maxima locations would be a practical method to accurately find the transition temperature! The curve $c_V^{\max}$ vs. $N^{-1/2}$ is better behaved, but it should be remarked, that a curve $c_V^{\max}$ vs. $N^{-1/3}$ looks equally nice {ref. 30}, and if one would plot $c_V^{\max}$ vs. $N^{-1/6}$ all data included in Fig. 16(a) would fall perfectly on a straight line—unfortunately there is no theoretical reason

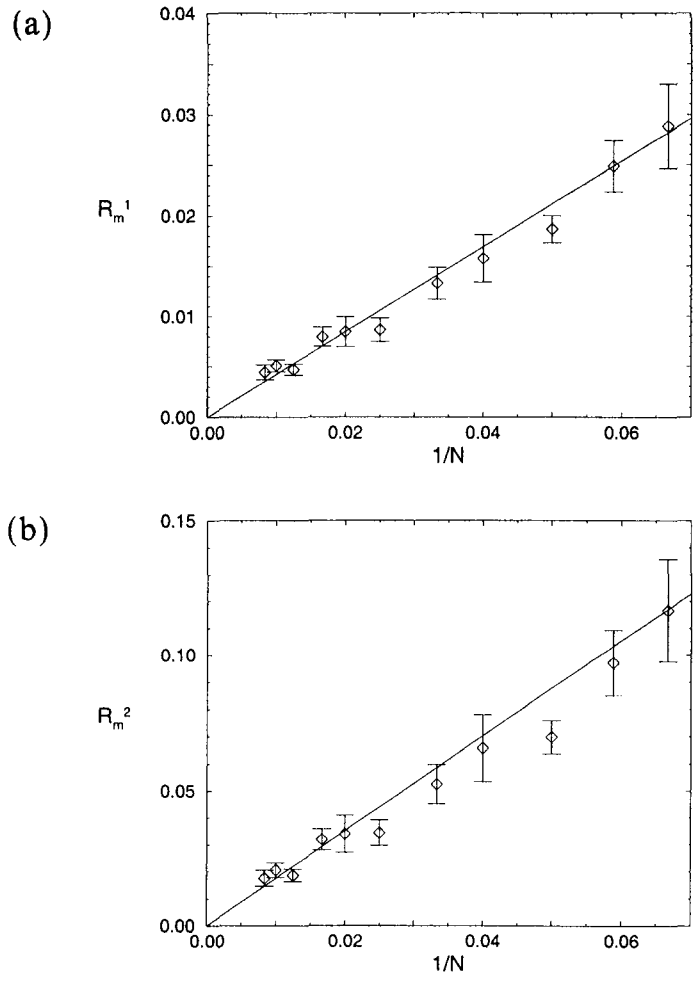

Fig. 18. Plot of the ratios R_{m^1} (a) and R_{m^2} (b) at $T = T_c$ versus $1/N$ for $p = 6$.

known to us to expect such an exponent, however. Rather a more plausible interpretation is that the first-order glass transition is rather weak (since q_{jump} is much smaller than unity) and hence rather large N may be required to establish the proper asymptotic behavior.

A rather interesting distinction concerns the ratios R_X characterizing the self-averaging properties: both R_u, R_{c_V} and R_{m^1}, R_{m^2} seem to exhibit strong self-averaging at T_c (Figs. 17, 18). The ratios R_{q^1} and R_{q^2}, on the other hand, even show a slight tendency to increase with N for large N, indicating that the asymptotic region has not quite been reached (Fig. 19).

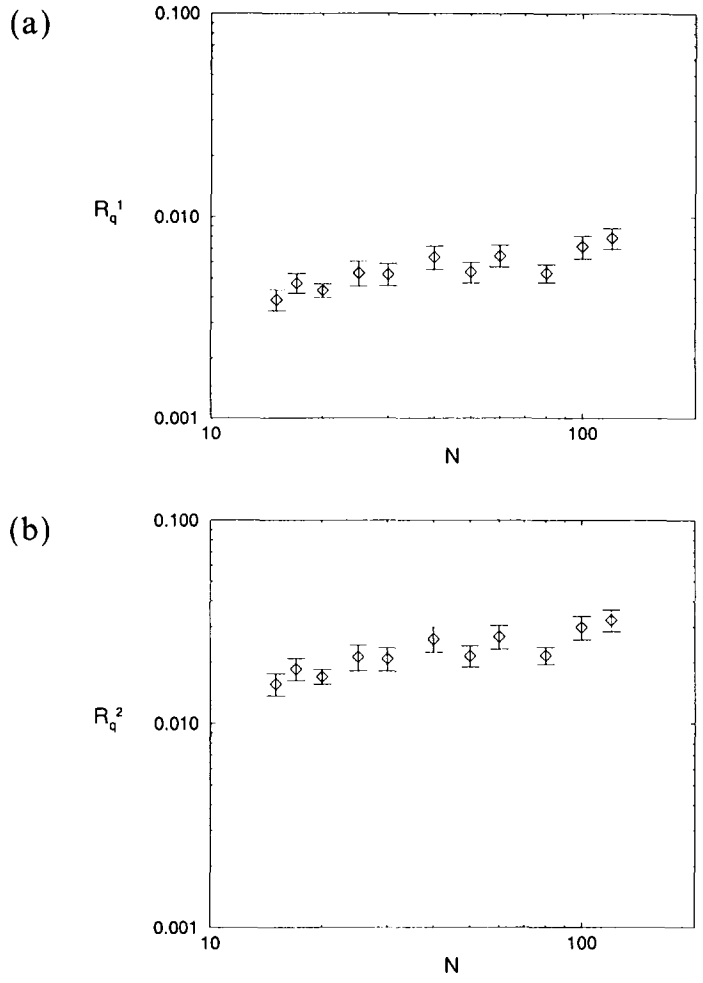

Fig. 19. Log-log plot of the ratios R_{q^1} (a) and R_{q^2} (b) for $T = T_c$ versus N for $p = 6$.

5. CONCLUDING REMARKS

In this paper we have addressed static properties of the p-state infinite-range Potts glass from the point of view of finite-size scaling, studying both $p=3$ and $p=6$. While for $p=3$ mean-field theories based on the replica method predict a second-order glass transition, for $p=6$ a first-order glass transition without latent heat is predicted. Our Monte Carlo results are compatible with these predictions. We have relied, however, on the knowledge of T_c from the mean-field theory, while the Monte Carlo data by themselves are not really so suitable to locate the transition temperature accurately. E.g., since the specific heat at T_c is finite in both models, extrapolation of the location of specific-heat maxima (which is one of the standard methods of locating phase transitions of standard type, of course) is not practical here. Another standard method, looking for common intersection points of the order parameter cumulant is not a successful approach here either: this is already seen from the amplitude factors in the asymptotic power laws for $q^{(k)}$ at T_c, which are for $p=3: q^{(2)} \approx 0.9 N^{-2/3}$, $q^{(4)} \approx 1.35 N^{-4/3}$, and hence g_4 {Eq. (24)} becomes $g_4 = 2\{3/2 - q^{(4)}/[q^{(2)}]^2\} \approx 0$, within the accuracy with which we could estimate these prefactors! Thus the behavior of g_4 near T_c is mostly controlled by corrections to finite-size scaling, and no unique intersection point is found. This behavior seems to differ appreciably from the infinite range Ising spin glass, where such analyses have had reasonable success. Another unsatisfactory feature of our results is that they cannot distinguish the difference in character of the transition for $p=3$ and for $p=6$.

An intriguing property that is not understood is the fact that for $p=3$ the ratios R_{m^k} relating to the self-averaging properties of the moments of the magnetization distribution seem to imply weak self-averaging only, while for $p=6$ strong self-averaging is found. In contrast, $[\langle m^k \rangle_{T_c}]_{\text{av}} \approx N^{-k/2}$ holds in both cases.

It hence would be very desirable if the replica theory could be extended to treat finite-size effects for the Potts glass as well, as was done for the Ising spin glass by Parisi *et al.*[24, 25] Such an extension to finite systems could be much more stringently tested than the thermodynamic limit, $N \to \infty$, for which our data do allow a tentative extrapolation, but there are still significant uncertainties. We hope that the present work will stimulate such an extension of the replica theory. Also the ratios characterizing self-averaging properties should be computed from such a treatment.

Another interesting extension of our model which must be left to future work is the extension to dynamics. Since the model is related to models of the structural glass transition, such an extension clearly would be

very interesting. A further topic that deserves study is the search for other systems which exhibit first-order transitions without latent heat. Our phenomenological theory for this case could then be put to another test.

APPENDIX: FINITE-SIZE SCALING FOR FIRST-ORDER TRANSITIONS WITHOUT A LATENT HEAT

In this appendix we speculatively consider various heuristic possibilities to describe first-order transitions without latent heat, without relying explicitly on the use of the replica theory to the Potts glass.[6, 7]

One possibility to obtain a first-order transition, where the order parameter jumps discontinuously but there is no latent heat, is to consider second order transitions with general exponents β, $\gamma \cdots$ and consider the limit $\beta \to 0$. The finite-size scaling relations (for systems with short range interactions in a (hyper-) cubic box of volume L^d) can be written as[21]

$$q = t^{\beta}\, \tilde{Q}(t\, L^{d/(\gamma+2\beta)}), \qquad \chi_{SG} = t^{-\gamma} \tilde{\chi}(t\, L^{d/(\gamma+2\beta)}) \tag{52}$$

where we have used the abbreviation $t = 1 - T/T_c$ and replaced the more standard factor $L^{1/\nu}$ (where ν is the correlation length exponent) by $L^{d/(\gamma+2\beta)}$, since then Eq. (52) holds also above the upper critical dimension d_u (where the hyperscaling relation $d\nu = \gamma + 2\beta$ no longer holds). The mean-field limit where spins interact independent of distance is obtained from Eq. (52) by identifying the volume L^d with the number of spins, N, i.e.

$$q = t^{\beta}\, \tilde{Q}(t\, N^{1/(\gamma+2\beta)}), \qquad \chi_{SG} = t^{-\gamma} \tilde{\chi}(t\, N^{1/(\gamma+2\beta)}) \tag{53}$$

It is seen that using the mean-field exponents $\gamma = 1$, $\beta = 1$ appropriate for spin glasses one obtains

$$q = t\, \tilde{Q}(t\, N^{1/3}), \qquad \chi_{SG} = t^{-1} \tilde{\chi}(t\, N^{1/3}) \tag{54}$$

As expected, these relations are equivalent to Eqs. (32), (34).

If we would assume that Eq. (53) holds also for a case with $\beta = 0$, one would conclude ($\beta = 0$)

$$q = \tilde{Q}(t\, N^{1/\gamma}), \qquad \chi_{SG} = t^{-\gamma} \tilde{\chi}(t\, N^{1/\gamma}) \xrightarrow{t \to 0} \chi_{SG} \propto N \tag{55}$$

It is seen that this treatment does not yield any information on finite-size corrections to the order parameter at T_c, since there simply $q = \tilde{Q}(0)$ is independent of N in the finite-size scaling limit.

Another possibility is to consider the standard finite-size scaling theory for first-order transitions.[21, 29, 36–38] There one starts from the fact that for

$T = T_c$ the free energies of the ordered (F_{ord}) and disordered (F_{dis}) phases are equal, F_c, and assumes that Taylor expansions can be written down both for $T > T_c$ and $T < T_c$, which we distinguish by superscripts $>$, $<$, see Fig. 20. In Fig. 20, we disregard the problem that in the replica theory the thermal equilibrium is described by a maximum rather than a minimum of the free energy (which would imply in Fig. 20(a), (b) the opposite sign of the curvature of the various branches, of course).

$$F_{dis}^{>} = F_c + \left(\frac{\partial F_{dis}^{>}}{\partial T}\right)_{T_c} (T - T_c) + \frac{1}{2}\left(\frac{\partial^2 F_{dis}^{>}}{\partial T^2}\right)_{T_c} (T - T_c)^2 + \cdots \quad (56)$$

$$F_{ord}^{>} = F_c + \left(\frac{\partial F_{ord}^{>}}{\partial T}\right)_{T_c} (T - T_c) + \frac{1}{2}\left(\frac{\partial^2 F_{ord}^{>}}{\partial T^2}\right)_{T_c} (T - T_c)^2 + \cdots \quad (57)$$

$$F_{dis}^{<} = F_c + \left(\frac{\partial F_{dis}^{<}}{\partial T}\right)_{T_c} (T - T_c) + \frac{1}{2}\left(\frac{\partial^2 F_{dis}^{<}}{\partial T^2}\right)_{T_c} (T - T_c)^2 + \cdots \quad (58)$$

$$F_{ord}^{<} = F_c + \left(\frac{\partial F_{ord}^{<}}{\partial T}\right)_{T_c} (T - T_c) + \frac{1}{2}\left(\frac{\partial^2 F_{ord}^{<}}{\partial T^2}\right)_{T_c} (T - T_c)^2 + \cdots \quad (59)$$

We now consider the free energy differences $\Delta F^{>} = F_{ord}^{>} - F_{dis}^{>} > 0$ and $\Delta F^{<} = F_{dis}^{<} - F_{ord}^{<} > 0$, which we have defined such that both of them are positive, and assuming that the ordered phase is stable at $T < T_c$, and the disordered one is stable at $T > T_c$. Considering now the situation that the latent heat is zero, we must have $(\partial F_{dis}^{>}/\partial T)_{T_c} = (\partial F_{ord}^{>}/\partial T)_{T_c} = (\partial F_{dis}^{<}/\partial T)_{T_c} = (\partial F_{ord}^{<}/\partial T)_{T_c}$, i.e., the free energy cannot have a kink at T_c, as it has in the case of a latent heat, but only a discontinuity in a higher derivative can occur. Therefore

$$\Delta F^{>} = \frac{1}{2}\left\{\left(\frac{\partial^2 F_{ord}^{>}}{\partial T^2}\right)_{T_c} - \left(\frac{\partial^2 F_{dis}^{>}}{\partial T^2}\right)_{T_c}\right\}(T - T_c)^2 + \cdots$$

$$\equiv \tilde{C}^{>}(T - T_c)^2 + \cdots \quad (60)$$

$$\Delta F^{<} = \frac{1}{2}\left\{\left(\frac{\partial^2 F_{dis}^{<}}{\partial T^2}\right)_{T_c} - \left(\frac{\partial^2 F_{ord}^{<}}{\partial T^2}\right)_{T_c}\right\}(T - T_c)^2 + \cdots$$

$$\equiv \tilde{C}^{<}(T - T_c)^2 + \cdots \quad (61)$$

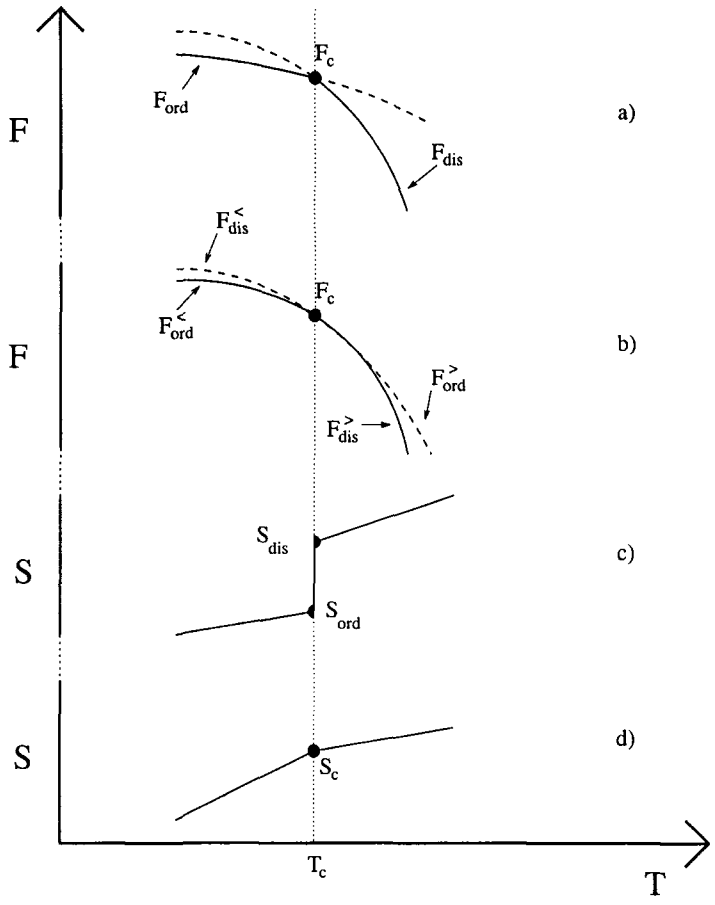

Fig. 20. Schematic variation of free energy F(a), (b) and entropy $S=-(\partial F/\partial T)_V$ (c), (d) with temperature at first order transitions, both for the case with a latent heat $E_{dis}-E_{ord}=(S_{dis}-S_{ord})/T_c$ (a), (c) and without it (b), (d). In the case with latent heat, free energies of the ordered and disordered branches F_{ord}, F_{dis} are equal at T_c ($F_{ord}=F_{dis}=F_c$) but differ already in order $(T-T_c)$, while in the case without latent heat both F and $(\partial F/\partial T)_V$ are equal in both branches at $T=T_c$, and only $(\partial^2 F/\partial T^2)_V$ at T_c differs. Note, however, that we must have $F^>_{dis}<F^>_{ord}$ for $T>T_c$ and simultaneously $F^<_{ord}<F^<_{dis}$ for $T<T_c$, which cannot happen if two regular functions touch tangentially at T_c: Then the function whose specific heat is larger would have the lower free energy at both sides of T_c. Thus a first order transition without latent heat must involve a singularity of at least one branch at T_c. In Eqs. (56)–(59) a jump singularity of the specific heat is assumed.

The weights with which the ordered and disordered phases appear above T_c and below T_c hence can be written as follows

$$W_{\text{dis}} \propto \exp[\Delta F^{>} N/(2k_B T)],$$
$$W_{\text{ord}} \propto \exp[-\Delta F^{>} N/(2k_B T)], \qquad T > T_c \tag{62}$$
$$W_{\text{dis}} \propto \exp[-\Delta F^{<} N/(2k_B T)],$$
$$W_{\text{ord}} \propto \exp[\Delta F^{<} N/(2k_B T)], \qquad T < T_c \tag{63}$$

Eqs. (62), (63) are still formally identical to the results of Vollmayr *et al.*[38] who allowed a nonzero latent heat $E_{\text{dis}} - E_{\text{ord}}$ and hence the free energy differences varied linear in $T - T_c$, $F_{\text{dis}} - F_{\text{ord}} = -(E_{\text{dis}} - E_{\text{ord}})(T - T_c)/T_c + \cdots$. While in this case with $E_{\text{dis}} - E_{\text{ord}} > 0$ in leading order the weights simply are[38]

$$W_{\text{dis}} \propto \exp\{(E_{\text{dis}} - E_{\text{ord}})(T - T_c)\, N/(2k_B T_c^2)\} \tag{64}$$
$$W_{\text{ord}} \propto \exp\{-(E_{\text{dis}} - E_{\text{ord}})(T - T_c)\, N/(2k_B T_c^2)\} \tag{65}$$

in the present case the quadratic variation of $\Delta F^{>}$, $\Delta F^{<}$ in $(T - T_c)$ leads to a different scaling behavior of the weights, namely for $T > T_c$

$$W_{\text{dis}} \propto \exp\{\tilde{C}^{>}(T - T_c)^2\, N/(2k_B T_c)\} \tag{66}$$
$$W_{\text{ord}} \propto \exp\{-\tilde{C}^{>}(T - T_c)^2\, N/(2k_B T_c)\} \tag{67}$$

and for $T < T_c$

$$W_{\text{dis}} \propto \exp\{-\tilde{C}^{<}(T - T_c)^2\, N/(2k_B T_c)\} \tag{68}$$
$$W_{\text{ord}} \propto \exp\{\tilde{C}^{<}(T - T_c)^2\, N/(2k_B T_c)\} \tag{69}$$

According to the theory developed in refs. 29, 36, and 38 these weight factors controlled both rounding and shifting of the transition (the order of magnitude of these effects is simply estimated by arguing that the argument of the exponential function in the region where the transition is rounded is of order unity!). From Eqs. (64), (65) one predicts a rounding of order $|T - T_c| \propto 1/N$ while Eqs. (66), (67) and (68), (69) predict a rounding of order $|T - T_c| \propto 1/\sqrt{N}$.

These conclusions are made more explicit considering the order parameter distribution, following ref. 38 using normalized weights h, $1-h$ {cf. Eq. (14) of ref. 38}

$$P_N(q) = h\, q^{p-2}\, \Omega_{p-1} \frac{N^{(p-1)/2}}{(2\pi k_B T \chi_{\text{dis}})^{(p-1)/2}} \exp\left\{-\frac{q^2 N}{2k_B T \chi_{\text{dis}}}\right\} + (1-h) \frac{N^{1/2}}{(2\pi k_B T \chi_{\text{ord}})^{1/2}} \exp\left\{-\frac{(q-q_{\text{jump}})^2 N}{2k_B T \chi_{\text{ord}}}\right\} \tag{70}$$

where we have assumed that we can treat the order parameter $q^{\mu\nu}$ of the spin glass analogous to the $(p-1)$-dimensional order parameter of the Potts ferromagnet, Ω_{p-1} being the surface area of a $(p-1)$-dimensional unit sphere, and χ_{dis}, χ_{ord} are the spin glass susceptibilities in the disordered and ordered phases at $T = T_c$ in the thermodynamic limit, respectively. The weakest point of this analogy is that some assumption on the degeneracy of the ordered phase of the spin glass is needed. The smallest possible degeneracy is that of the corresponding Potts ferromagnet, i.e., p (this assumption is probably true near the lower critical dimensionality but not for the mean-field Potts glass). Then

$$\begin{aligned} h &= W_{\text{dis}}/(W_{\text{dis}} + p\, W_{\text{ord}}) \\ &= \begin{cases} 1/\{1 + p \exp[-\tilde{C}^{>}(T-T_c)^2 N/k_B T_c]\} \equiv h^{>}, & T > T_c \\ 1/\{1 + p \exp[\tilde{C}^{<}(T-T_c)^2 N/k_B T_c]\} \equiv h^{<}, & T < T_c \end{cases} \end{aligned} \tag{71}$$

It is clear that Eq. (71) does not reduce to weights of the ordered and disordered phases $1-h^{<} \propto (1 - T/T_c)$, $h^{<} \propto T/T_c$ in the thermodynamic limit, that the replica theory predicts.[6, 7] It is not clear to us how one has to modify Eqs. (64)–(70) in order to obtain the results of the latter theory.

In ref. 38 it was pointed out, that the parameters of this model calculation can be scaled out by defining a renormalized "volume"

$$n = q_{\text{jump}}^2\, N/(2k_B T_c \chi_{\text{ord}}) \tag{72}$$

as well as a renormalized temperature scale, which in ref. 38 was written as

$$\Delta\tilde{T} = A(T - T_c), \qquad A = (E_{\text{ord}} - E_{\text{dis}})\, \chi_{\text{ord}}/(q_{\text{jump}}^2\, T_c) \tag{73}$$

while in the present case where $A \equiv 0$ we rather have a variable

$$(\delta\tilde{T})^2 = B_{\pm}(T - T_c)^2, \qquad B_{\pm} = \pm\tilde{C}^{\gtrless}\chi_{\text{ord}}/q_{\text{jump}}^2 \tag{74}$$

and then all moments $\langle q^k \rangle$ only depend on one additional parameter $x = \sqrt{\chi_{\text{dis}}/\chi_{\text{ord}}}$. Thus we recognize that the treatment of ref. 38 to a large extent can be carried over, if we consider the (nonlinear!) transformation of the temperature scale from Eq. (73) to Eq. (74). In particular, we conclude from this that the cumulant g_4 considered in Eq. (24) still should have a nearly universal intersection point for N so large that also $n \gg 1$ {Eq. (72)} and a minimum for $T > T_c$. We predict according to ref. 38, using Eqs. (73), (74), that the position of this minimum should scale as

$$T_{\min} - T_c \propto 1/\sqrt{N} \qquad \text{if} \quad n \gg 1 \tag{75}$$

Note, however, that due to the smallness of q_{jump} {Eq. (36)} it is doubtful whether the condition $n \gg 1$ can be met in practice. And while the deviations of intersections between $g_4(N)$, $g_4(2N)$ in the case $E_{\text{ord}} - E_{\text{dis}} \neq 0$ scale like $T_{\text{inter}}(N, 2N) - T_c \propto 1/N^2$, we here expect only a scaling like $1/N$, $T_{\text{inter}}(N, 2N) - T_c \propto 1/N$ in the present case.

While with respect to finite-size effects on the order parameter the lack of any latent heat thus simply expands the temperature scale on which the transition is smeared out from $1/N$ to $1/\sqrt{N}$, for the specific heat the phenomena are naturally more drastic: In the case where a latent heat is present we have

$$C_V^{\max}/k_B = (E_{\text{dis}} - E_{\text{ord}})^2 N/(2k_B T_c)^2 + (C_{\text{dis}} + C_{\text{ord}})/2 + \tfrac{1}{2}[C_{\text{dis}} - C_{\text{ord}} - (E_{\text{dis}} - E_{\text{ord}})/(k_B T_c)] \ln p + \mathcal{O}(1/N) \tag{76}$$

where the first term represents the smeared delta-function singularity, and the next term, the "background" specific heat (where C_{dis}, C_{ord} are the specific heats of the two phases at T_c in the limit $N \to \infty$) hence is a relative correction of order $1/N$ only. In our case such a finite term is the leading term. In order to derive the specific heat in the transition region, we write the internal energy of the finite system $E_N^<$, $E_N^>$ below and above T_c as a weighted average over both phases,

$$E_N^< = h^< E_{\text{dis}}^< + (1 - h^<) E_{\text{ord}}^<, \qquad T < T_c \tag{77}$$

$$E_N^> = h^> E_{\text{dis}}^> + (1 - h^>) E_{\text{ord}}^>, \qquad T > T_c \tag{78}$$

Using $E = F - T(\partial F/\partial T)_V$ we obtain from Eqs. (56)–(59)

$$E_{\text{dis}}^> = F_c - T_c \left(\frac{\partial F_{\text{dis}}^>}{\partial T}\right)_{T_c} + \frac{1}{2}(T_c^2 - T^2)\left(\frac{\partial^2 F_{\text{dis}}^>}{\partial T^2}\right)_{T_c} + \cdots \tag{79}$$

$$E_{\text{ord}}^> = F_c - T_c \left(\frac{\partial F_{\text{ord}}^>}{\partial T}\right)_{T_c} + \frac{1}{2}(T_c^2 - T^2)\left(\frac{\partial^2 F_{\text{ord}}^>}{\partial T^2}\right)_{T_c} + \cdots \tag{80}$$

$$E_{\text{dis}}^{<} = F_c - T_c \left(\frac{\partial F_{\text{dis}}^{<}}{\partial T} \right)_{T_c} + \frac{1}{2} (T_c^2 - T^2) \left(\frac{\partial^2 F_{\text{dis}}^{<}}{\partial T^2} \right)_{T_c} + \cdots \tag{81}$$

$$E_{\text{ord}}^{<} = F_c - T_c \left(\frac{\partial F_{\text{ord}}^{<}}{\partial T} \right)_{T_c} + \frac{1}{2} (T_c^2 - T^2) \left(\frac{\partial^2 F_{\text{ord}}^{<}}{\partial T^2} \right)_{T_c} + \cdots \tag{82}$$

The specific heat then is found from

$$\begin{aligned} C_N^{<} &= \frac{dE_N^{<}}{dT} = h^{<} \frac{dE_{\text{dis}}^{<}}{dT} + (1 - h^{<}) \frac{dE_{\text{ord}}^{<}}{dT} + \frac{dh^{<}}{dT} (E_{\text{dis}}^{<} - E_{\text{ord}}^{<}) \\ &= -T \left(\frac{\partial^2 F_{\text{ord}}^{<}}{\partial T^2} \right)_{T_c} - \tilde{C}^{<} \left[2T h^{<} + (T^2 - T_c^2) \frac{dh^{<}}{dT} \right] \end{aligned} \tag{83}$$

$$C_N^{>} = -T \left(\frac{\partial^2 F_{\text{ord}}^{>}}{\partial T^2} \right)_{T_c} + \tilde{C}^{>} \left[2T h^{>} + (T^2 - T_c^2) \frac{dh^{>}}{dT} \right] \tag{84}$$

From Eq. (71) we find for $T > T_c$ in terms of $x \equiv \tilde{C}^{>} (T - T_c)^2 N / k_B T_c$ that $h^{>} = (1 + p\, e^{-x})^{-1}$, and hence

$$\frac{dh^{>}}{dT} = \frac{dh^{>}}{dx} \frac{dx}{dT} = \frac{dh^{>}}{dx} \frac{2\tilde{C}^{>} (T - T_c) N}{k_B T_c}, \qquad \frac{dh^{>}}{dx} = \frac{p\, e^{-x}}{(1 + p\, e^{-x})^2} \tag{85}$$

and similarly for $T < T_c$, using then $x \equiv \tilde{C}^{<} (T - T_c)^2 N / k_B T_c$ and $h^{<} = (1 + p\, e^{x})^{-1}$

$$\frac{dh^{<}}{dT} = \frac{dh^{<}}{dx} \frac{dx}{dT} = \frac{dh^{<}}{dx} \frac{2\tilde{C}^{<} (T - T_c) N}{k_B T_c}, \qquad \frac{dh^{<}}{dx} = \frac{-p\, e^{x}}{(1 + p\, e^{x})^2} \tag{86}$$

From Eqs. (85), (86) we see that $C_N^{<}$, $C_N^{>}$ can be rewritten as

$$C_N^{<} = -T \left(\frac{\partial^2 F_{\text{ord}}^{<}}{\partial T^2} \right)_{T_c} - 2\tilde{C}^{<} \left[T h^{<} + (T + T_c)\, x \frac{dh^{<}}{dx} \right] \tag{87}$$

$$C_N^{>} = -T \left(\frac{\partial^2 F_{\text{ord}}^{>}}{\partial T^2} \right)_{T_c} + 2\tilde{C}^{>} \left[T h^{>} + (T + T_c)\, x \frac{dh^{>}}{dx} \right] \tag{88}$$

Of course, a necessary consistency condition of our description is that for $T = T_c$ the specific heat is continuous, $C_N^{<}|_{T_c} = C_N^{>}|_{T_c}$. This requires, noting that at T_c we have $h^{<} = h^{>} = (1 + p)^{-1}$,

$$\left(\frac{\partial^2 F_{\text{ord}}^{>}}{\partial T^2} \right)_{T_c} = \left(\frac{\partial^2 F_{\text{ord}}^{<}}{\partial T^2} \right)_{T_c} + 2(\tilde{C}^{>} + \tilde{C}^{<})/(1 + p) \tag{89}$$

For $T > T_c$ and large x we have $h^> \to 1$, $dh^>/dx \to 0$ and hence

$$C_N^> = -T\left(\frac{\partial^2 F_{\text{ord}}^>}{\partial T^2}\right)_{T_c} + 2T\tilde{C}^> = -T\left(\frac{\partial^2 F_{\text{dis}}^>}{\partial T^2}\right)_{T_c} \tag{90}$$

as it should be. Similarly, for $T < T_c$ and large x we have $h^< \to 0$, and thus $C_N^< = -T(\partial^2 F_{\text{ord}}^</\partial T^2)_{T_c}$ remains as required. Thus Eqs. (87), (88) describe the smooth crossover from $C_\infty^> = -T(\partial^2 F_{\text{dis}}^>/\partial T^2)_{T_c}$ to $C_\infty^< = -T(\partial^2 F_{\text{ord}}^</\partial T^2)_{T_c}$, i.e., the jump of the specific heat from one finite value to another finite value is rounded on the scale of $\Delta T \propto 1/\sqrt{N}$, as is obvious from the above definitions of x. Since for large N this temperature interval is rather narrow, we may replace T by T_c in the square brackets in Eqs. (87), (88), to obtain

$$C_N^< \approx -T_c\left(\frac{\partial^2 F_{\text{ord}}^<}{\partial T^2}\right)_{T_c} - 2\tilde{C}^< T_c\left[h^< + 2x\frac{dh^<}{dx}\right] \tag{91}$$

and similarly for $C_N^>$. Using Eqs. (85), (86), we find that the square bracket can be written as

$$f^<(x) \equiv h^< + 2x\frac{dh^<}{dx} = \frac{1 + p\,e^x - 2p\,x\,e^x}{(1 + p\,e^x)^2} \tag{92}$$

which shows that $C_N^<$ has a maximum at $x_m > 0$ given by the following transcendental equation

$$3 + 2x_m + 3p\,e^{x_m} - 2p\,x_m\,e^{x_m} = 0 \tag{93}$$

Since the relation between T and x is given by the quadratic equation $x = \tilde{C}^<(T - T_c)^2 N/k_B T_c$, however, the two signs of the solution for $T_m - T_c$ corresponding to x_m would imply two maxima of the specific heat both above and below T_c. But Eqs. (91)–(93) should be used for $T < T_c$ only. For $T > T_c$, Eq. (88) implies near T_c

$$C_N^> \approx -T_c\left(\frac{\partial^2 F_{\text{ord}}^>}{\partial T^2}\right)_{T_c} + 2\tilde{C}^> T_c\left[h^> + 2x\frac{dh^>}{dx}\right] \tag{94}$$

with

$$f^>(x) \equiv h^> + 2x\frac{dh^>}{dx} = \frac{1 + p\,e^{-x} + 2p\,x\,e^{-x}}{(1 + p\,e^{-x})^2} = f^<(-x) \tag{95}$$

which has a maximum at $x'_m > 0$. {Note that for $T > T_c$ the constant $\tilde{C}^>$ replaces $-\tilde{C}^<$, cf. Eq. (71): Since both constants $\tilde{C}^>$, $\tilde{C}^<$ have been defined such that they are positive, cf. Fig. 20(b) and Eqs. (60), (61), the two solutions $x_m > 0$ and $-x'_m < 0$ are the minimum and maximum of $f^<(x)$, respectively.} Hence we conclude that the specific heat has two maxima at $T_m < T_c$ and $T'_m > T_c$, given in terms of x_m and x'_m {Eq. (93)} as

$$T_m - T_c = -(k_B T_c x_m / \tilde{C}^< N)^{1/2} \tag{96}$$

$$T'_m - T_c = (k_B T_c x'_m / \tilde{C}^> N)^{1/2} \tag{97}$$

i.e., the specific heat has finite maxima shifted from T_c by a $N^{-1/2}$ correction.

For a typical set of parameters (e.g., $p = 6$, $T_c = 1$, $(\partial^2 F^>_{\text{dis}}/\partial T^2)_{T_c} = -1.5$, $(\partial^2 F^<_{\text{ord}}/\partial T^2)_{T_c} = -0.5$, $(\partial^2 F^<_{\text{dis}}/\partial T^2)_{T_c} = -0.3$, and $(\partial^2 F^>_{\text{ord}}/\partial T^2)_{T_c} = -0.3$ (using Eq. (89)), however, the maximum at $T_m < T_c$ turns out to be so shallow that it is hardly visible and therefore difficult to detect with noisy Monte Carlo data. For an illustration see Fig. 21. In any quantitative comparison with the Monte Carlo data it should be kept in mind, of course, that Eqs. (91)–(95) are leading-order approximations which can only be trusted in the limit $N \to \infty$, $T \approx T_c$. And since in the present case, $1/\sqrt{N}$ is the relevant parameter, the asymptotic region is reached much slowlier than for a standard first-order phase transition with a non-vanishing latent heat where the finite-size scaling is governed by $1/N$.

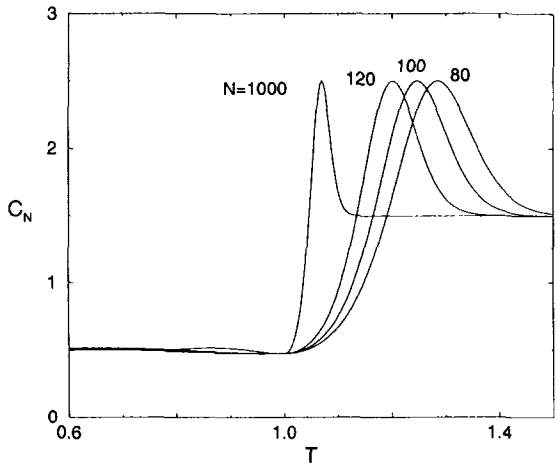

Fig. 21. Leading-order prediction for the specific heat C_N according to Eqs. (91)–(95) for $p = 6$ with $T_c = 1$, $(\partial^2 F^>_{\text{dis}}/\partial T^2)_{T_c} = -1.5$, $(\partial^2 F^<_{\text{ord}}/\partial T^2)_{T_c} = -0.5$, $(\partial^2 F^<_{\text{dis}}/\partial T^2)_{T_c} = -0.3$, and $(\partial^2 F^>_{\text{ord}}/\partial T^2)_{T_c} = -0.3$ (using Eq. (89)). The peak at $T_m < T_c$ is strongly suppressed because $-f^<(x_m) \approx 0.0682$ is much smaller than $f^<(-x'_m) \approx 1.8342$ ($x_m \approx 1.6040$, $x'_m \approx 2.9249$).

This conclusion can be obtained in a rather different way, generalizing the description of first-order transitions developed by Borgs *et al.*[36] Then the partition function is written as

$$\begin{aligned} Z(T, N) &= p \exp[-NF_{\text{ord}}(T)/k_B T] + \exp[-NF_{\text{dis}}(T)/k_B T] \\ &\quad + \text{exponentially small terms} \\ &= 2\sqrt{p} \exp\{-N[F_{\text{ord}}(T) + F_{\text{dis}}(T)]/2k_B T\} \cosh(y) \end{aligned} \tag{98}$$

where

$$y = N\Delta F/(2k_B T) + \tfrac{1}{2} \ln p, \qquad \Delta F = F_{\text{dis}} - F_{\text{ord}} \tag{99}$$

Note, however, that also in this formulation ΔF for $T > T_c$ and for $T < T_c$ must be different, cf. Fig. 20 and Eqs. (56)–(61). Using $\beta \equiv 1/k_B T$ one finds for the energy per spin

$$E = -(1/N) \frac{\partial \ln Z}{\partial \beta} = [E_{\text{ord}}(T) + E_{\text{dis}}(T)]/2 - \frac{1}{2} \Delta E \tanh(y) \tag{100}$$

where $\Delta E = E_{\text{dis}} - E_{\text{ord}}$. The specific heat then becomes

$$C = -\beta^2 \frac{\partial E}{\partial \beta} = \beta^2 N(\langle E^2 \rangle - \langle E \rangle^2) = \beta^2 \mu^{(2)} \tag{101}$$

where the abbreviation is introduced

$$\mu^{(2)} = N(\Delta E/2)^2/\cosh^2(y) + [\mu_{\text{ord}}^{(2)} + \mu_{\text{dis}}^{(2)}]/2 - [\Delta\mu^{(2)}/2] \tanh(y) \tag{102}$$

where $\mu_{\text{ord}}^{(2)}$, $\mu_{\text{dis}}^{(2)}$ are the normalized specific heats of the pure ordered or disordered phases, respectively, and $\Delta\mu^{(2)} = \mu_{\text{dis}}^{(2)} - \mu_{\text{ord}}^{(2)}$. For $\Delta\hat{E} \equiv \Delta E(\beta_c) \neq 0$, the maximum location β_{max} can be systematically expanded as $\beta_{\max} = \beta_c + a_1/N + \cdots$, expanding all quantities around β_c ($\Delta\beta \equiv \beta - \beta_c$),

$$y = \frac{1}{2} \ln p + N \left\{ \frac{\Delta\hat{E}}{2} \Delta\beta - \frac{1}{2} \frac{\Delta\hat{\mu}^{(2)}}{2} (\Delta\beta)^2 + \cdots \right\} \tag{103}$$

$$\Delta E = \Delta\hat{E} - \Delta\hat{\mu}^{(2)} \Delta\beta + \cdots, \qquad \mu^{(2)} = \hat{\mu}^{(2)} - \hat{\mu}^{(3)} \Delta\beta + \cdots, \text{ etc.} \tag{104}$$

where the "hat" again indicates quantities evaluated at β_c. For $\Delta\hat{E} \neq 0$ (nonzero latent heat) the maximum of $\mu^{(2)}$ in Eq. (102) is found for $y = 0$, of course, and then Eq. (103) yields the well-known shift inversely proportional to N, $\Delta\beta = (\ln p/\Delta\hat{E})/N$. For $\Delta\hat{E} = 0$, however, $y = 0$ is not the solution,

since then all terms in Eq. (102) are of the same order. In leading order Eq. (102) then yields

$$\mu^{(2)} \approx N[\Delta\mu^{(2)}\Delta\beta/2]^2/\cosh^2[\ln p/2 - N\Delta\hat{\mu}^{(2)}(\Delta\beta)^2/4] + \frac{1}{2}[\hat{\mu}^{(2)}_{\text{ord}} + \hat{\mu}^{(2)}_{\text{dis}}] - \frac{\Delta\hat{\mu}^{(2)}}{2}\tanh[\ln p/2 - N\Delta\hat{\mu}^{(2)}(\Delta\beta)^2/4] \quad (105)$$

Abbreviating

$$\xi = N\Delta\hat{\mu}^{(2)}(\Delta\beta)^2/4 \quad (106)$$

Eq. (105) can be written as

$$\mu^{(2)} = \Delta\hat{\mu}^{(2)}\left[\xi/\cosh^2(\ln p/2 - \xi) - \frac{\tanh(\ln p/2 - \xi)}{2} + \frac{\hat{\mu}^{(2)}_{\text{ord}} + \hat{\mu}^{(2)}_{\text{dis}}}{2\Delta\hat{\mu}^{(2)}}\right] \quad (107)$$

Since the last term is a constant, the maximum of $\mu^{(2)}$ is found from $d\mu^{(2)}/d\xi = 0$ or

$$g(\xi) = 3 + 4\xi\tanh(\ln p/2 - \xi) = 0 \quad (108)$$

With a little algebra Eq. (108) can be reduced to Eq. (93), identifying $\xi = -x_m/2$.

ACKNOWLEDGMENTS

O. D. would like to thank the Regionales Hochschulrechenzentrum Kaiserslautern for generous allocation of Cray time. W. J. acknowledges support from the Deutsche Forschungsgemeinschaft (DFG) through a Heisenberg Fellowship. Partial support from the DFG via Sonderforschungsbereich 262/D1 is also gratefully acknowledged, as well as support from the German Israeli Foundation (GIF No. I-0438-145.07/95). We thank E. Domany and A. Aharony for stimulating discussions.

REFERENCES

1. K. Binder and A. P. Young, *Rev. Mod. Phys.* **58**:801 (1986).
2. M. Mezard, G. Parisi, and M. Virasoro, *Spin Glass Theory and Beyond* (World Scientific, Singapore, 1987).
3. K. H. Fischer and J. Hertz, *Spin Glasses* (Cambridge University Press, Cambridge, 1991).
4. D. S. Stein, *Spin Glasses and Biology* (World Scientific, Singapore, 1992).
5. D. Elderfield and D. Sherrington, *J. Phys. C* **16**:L491, L971, L1169 (1983).

6. D. J. Gross, I. Kanter, and H. Sompolinsky, *Phys. Rev. Lett.* **55**:304 (1985).
7. G. Cwilich and T. R. Kirkpatrick, *J. Phys. A* **22**:4971 (1989).
8. G. Cwilich, *J. Phys. A* **23**:5029 (1990).
9. R. Pirc and B. Tadic, *Phys. Rev. B* **54**:7121 (1996).
10. K. Binder and J. D. Reger, *Adv. Phys.* **41**:547 (1992).
11. K. Binder, in *Spin Glasses and Random Fields*, A. P. Young, ed. (World Scientific, Singapore, 1998), p. 99.
12. U. T. Höchli, K. Knorr, and A. Loidl, *Adv. Phys.* **39**:405 (1990).
13. F. Y. Wu, *Rev. Mod. Phys.* **54**:235 (1982); **55**:315(E) (1983).
14. T. R. Kirkpatrick and P. G. Wolynes, *Phys. Rev. B* **35**:3072; **36**:8552 (1987).
15. T. R. Kirkpatrick and D. Thirumalai, *Phys. Rev. B* **36**:5388; **37**:5342 (1987); D. Thirumalai and T. R. Kirkpatrick, *Phys. Rev. B* **38**:4881 (1988).
16. W. Götze and L. Sjögren, *Rep. Progr. Phys.* **55**:241 (1992).
17. M. Scheucher and J. D. Reger, *Z. Phys. B* **91**:383 (1993).
18. M. E. Fisher, in *Critical Phenomena, Proc. 1970 Enrico Fermi International School on Physics*, M. S. Green, ed. (Academic, New York, 1971), p. 1.
19. M. N. Barber, in *Phase Transitions and Critical Phenomena*, Vol. 8, C. Domb and J. L. Lebowitz, eds. (Academic, New York, 1983), p. 145.
20. V. Privman (ed.), *Finite Size Scaling and Numerical Simulation of Statistical Systems* (World Scientific, Singapore, 1990).
21. K. Binder, *Ferroelectrics* **73**:43 (1987); in *Computational Methods in Field Theory*, H. Gausterer and C. B. Lang, eds. (Springer, Berlin, 1992), p. 59.
22. A. P. Young and S. Kirkpatrick, *Phys. Rev. B* **25**:440 (1982).
23. G. Parisi, F. Ritort, and F. Slanina, *J. Phys. A* **26**:247,3775 (1993).
24. G. Parisi and F. Ritort, *J. Phys. A* **26**:6711 (1993); J. C. Ciria, G. Parisi, and F. Ritort, *J. Phys. A* **26**:6731 (1993).
25. B. O. Peters, B. Dünweg, K. Binder, M. d'Onorio de Meo, and K. Vollmayr, *J. Phys. A* **29**:3503 (1996).
26. S. Wiseman and E. Domany, *Phys. Rev. E* **52**:3469 (1995).
27. A. Aharony and A. B. Harris, *Phys. Rev. Lett.* **77**:3700 (1996).
28. R. K. P. Zia and D. J. Wallace, *J. Phys. A* **8**:1495 (1975).
29. M. S. S. Challa, D. P. Landau, and K. Binder, *Phys. Rev. B* **86**:1841 (1986).
30. O. Dillmann, Diplomarbeit (Universität Mainz, 1997), unpublished.
31. M. Scheucher, J. D. Reger, K. Binder, and A. P. Young, *Phys. Rev. B* **42**:6881 (1990).
32. M. Suzuki, *Progr. Theor. Phys.* **58**:1157 (1977).
33. M. Aizenman, *Nucl. Phys. B* **485**:551 (1997).
34. C. Borgs, J. Chayes, H. Kerten, and J. Spencer, "The birth of the infinite cluster: Finite size scaling in percolation" (1997), preprint.
35. C. Fortuin and P. Kasteleyn, *Physica* **57**:536 (1972).
36. C. Borgs and R. Kotecký, *J. Stat. Phys.* **61**:79 (1991); C. Borgs, R. Kotecký, and S. Miracle-Solé, *J. Stat. Phys.* **62**:529 (1991).
37. W. Janke, *Phys. Rev. B* **47**:14757 (1993).
38. K. Vollmayr, J. D. Reger, M. Scheucher, and K. Binder, *Z. Phys. B* **91**:113 (1993).
39. A. Milchev, K. Binder, and D. W. Heermann, *Z. Phys. B* **63**:521 (1986).
40. A. M. Ferrenberg and R. H. Swendsen, *Phys. Rev. Lett.* **61**:2635 (1988); **63**:1195 (1989).
41. H. Müller-Krumbhaar and K. Binder, *J. Stat. Phys.* **8**:1 (1973).
42. A. M. Ferrenberg, D. P. Landau, and K. Binder, *J. Stat. Phys.* **63**:867 (1991).
43. W. Janke, in *Computational Physics: Selected Methods, Simple Exercises, Serious Applications*, K. H. Hoffmann and M. Schreiber, eds. (Springer, Berlin, 1996), p. 10.